The Population of the Trans-Neptunian Region

Paul R. Weissman
Earth and Space Sciences Division
Jet Propulsion Laboratory
Pasadena, CA 91109

Harold F. Levison
Space Sciences Division
Southwest Research Institute
Boulder, CO 80302

Send all correspondence to:
Dr. P. R. Weissman
Jet Propulsion Laboratory
Mail stop 183-601
4800 Oak Grove Drive
Pasadena, CA 91109

Phone: (818) 354-2636
Fax: (818) 393-4605
E-mail: pweissman@issac.jpl.nasa.gov

Submitted to *Pluto-Charon*, University of Arizona Press

Abstract

The Pluto Charon system orbits the Sun in the trans-Neptunian region, at the edge of the planetary system. Because of their low masses, Pluto and Charon are unable to clear this zone of heliocentric space of small bodies, and thus they share it with two large cometary reservoirs, the Oort cloud and the Kuiper belt. The population and dynamics of Oort cloud comets in this region are not well defined. Contributing to the uncertainty is our relatively poor knowledge of the population and dynamics of the inner Oort cloud, which has been suggested but never detected. In contrast, major advances have been made in recent years in understanding the dynamics of the Kuiper belt, and observational programs to detect the Kuiper belt population have been highly successful. Like the asteroid belt, the dynamical structure of the Kuiper belt is sculpted by mean motion and secular resonances with the giant planets. It appears that most if not all Kuiper belt objects interior to -- 40 AU are locked in mean motion resonances with Neptune, just as the Pluto Charon binary is, while those beyond 40 AU are mostly confined to low eccentricity, non-resonant orbits near the ecliptic plane. The size distribution of the Kuiper belt objects is complex, and likely follows a broken power law, similar to that proposed for the long-period comets. Pluto Charon can also interact with objects in Trojan-type, 1:1 librations with Neptune. No clearly identifiable members of that population have yet been detected, though there do exist orbits in the Neptune Trojan region which are stable over the lifetime of the solar system. Pluto Charon are best viewed as the largest end-members of Inc. Kuiper belt population, rather than as an independent planet-satellite system.

I. Introduction

The Pluto-Charon binary exists at a unique location in the solar system, at the edge of the known planetary system. Because of its location and its relatively small mass, the Pluto-Charon binary is not capable of dynamically clearing its orbital zone of smaller objects, as has been done by all of the other planets over the history of the solar system. As a consequence, Pluto and Charon are not alone; they share their zone with the two major cometary reservoirs, the Oort cloud and the Kuiper belt, and possibly also with objects locked in Trojan-type resonances with

Neptune.

This chapter will describe the environment of the trans-Neptunian region, the region in which Pluto and Charon orbit the Sun. We define the trans-Neptunian region as extending from the near-circular orbit of Neptune at 30 AU, to 50 AU, just beyond Pluto's aphelion. It is objects in this region which have played a role in the formation of Pluto and Charon, and their subsequent impact and perturbation history. We include in our definition objects on Neptune-crossing orbits that are stable because they are locked in mean motion resonances with Neptune. It is also within this zone that Neptune is capable of acting as the major perturber of small bodies. Note that some of the populations of objects which we will discuss, such as the Oort cloud and the Kuiper belt, extend well beyond the defined boundaries of this region. Our focus in this chapter will be on discussing them in this region and their likely interactions with Pluto and Charon.

The Pluto Charon binary is distinctly different in both size and composition from the gas giant planets interior to it, and likely bears a far greater resemblance to the smaller icy objects which have been recently discovered in orbits beyond Neptune (Jewitt and Luu 1995; also see Weissman 1995a, for a review). Thus, it may be far more accurate to characterize Pluto and Charon as the largest known members of a numerous population of objects that grew in the trans-Neptunian region, rather than as an isolated planet-satellite system that gravitationally dominates its region of the solar system.

Although our knowledge of the trans-Neptunian zone is at best modest, we know that there are several populations that inhabit and/or transit this region of the solar system:

• It is obvious that long-lived comets from the Oort cloud must pass through the trans-Neptunian region on their way in and out of the planetary system, but the detailed flux of comets in the outer solar system is not well quantified. Uranus and Neptune are not sufficiently massive to eject comets from the solar system, and thus comets from the dynamically active outer Oort cloud and the unseen but much denser inner Oort cloud traverse this region fairly freely.

• Although speculation on the existence of a trans-Neptunian comet belt dates back almost 50 years (Edgeworth 1949; Kuiper 1951), serious work on the topic did not start until Fernández (1980) invoked it as a possible source reservoir for the short-period comets (those with orbital periods < 200 years). Dynamical simulations by Duncan et al. (1988) and Quinn et al. (1990) showed that a comet belt beyond Neptune is the most plausible source for the low

inclination, Jupiter-family short-period comets (see Levison 1995 for a recent review). Duncan et al. (1988) suggested the name "Kuiper belt" for this population, in recognition of Kuiper's 1951 paper suggesting it.[1] The first Kuiper belt object, 1992 QB_1, was discovered by Jewitt and Luu in 1992. Since then a total of 28 trans-Neptunian objects with radii ≥ 50 km have been found by ground-based searches (e.g., Williams et al. 1993; Jewitt and Luu 1995), and ~30 Halley sized objects have been found using the Hubble Space Telescope (HST, Cochran et al, 199s).

- Several dynamical studies have suggested that Neptunian Trojan asteroids locked in 1:1 resonant orbits with Neptune might be stable for periods of at least 2×10^7 to 2×10^8 years (Mikkola and Innanen 1992; Holman and Wisdom 1993). Although Pluto and Charon cannot make close approaches to Neptune because of the 2:3 resonance, they regularly pass through the regions that would be occupied by Trojan librators ahead and behind Neptune in its orbit.

- Considerable efforts have been devoted in the last several decades to the search for another planet beyond Pluto, as a means of explaining the purported perturbations on the orbits of Uranus and Neptune. However, Standish (1993) showed that the motion of both Uranus and Neptune could be fit without any additional perturbers, and previous discrepancies in their motion were the result of poor star catalogs, inaccurate masses of the planets, and other observational errors. Observational searches have ruled out any bodies comparable to (or larger than) the size of Pluto in low eccentricity orbits within 60 AU of the Sun.

These topics will be discussed in more detail in the following sections. Section 2 describes observational searches of the outer solar system and the discovery of the Kuiper belt objects. Section 3 reviews estimates of the flux of long-period comets from the Oort cloud through the trans-Neptunian region. Section 4 considers dynamical studies of the motion of objects in the Kuiper belt and their kmp,-term stability. Section 5 examines detection of the Kuiper belt due to its gravitational effects on spacecraft passing through the region, and other means of estimating the population of the trans-Neptunian region. Section 6 discusses the size [distribution of comets both in the Kuiper belt and the Oort cloud, Section 7 will consider Neptune Trojans. Section 8 summarizes our conclusions and discusses open questions

[1] Although Edgeworth (1949) also suggested a trans-Neptunian comet belt, his paper was essentially unknown to cometary dynamicists in the 19"/0's and 80's. Edgeworth even suggested that the belt might be a source of observable comets.

concerning the trans-Neptunian region.

Stud y of the trans-Neptunian region is still a very young field, both from the point of view of the observational searches which have. been made to date., and the computational studies of the dynamics of bodies in this region. Thus, some of what we discuss in the following sections is speculative, and much of it is likely to change rapidly in the coming year-s as this field matures and more data becomes available.

2. Observational Searches of the Outer Solar System

The greatest areal search for trans-Neptunian objects is that by Tombaugh (1961) which covered the entire sky north of -40° declination to B magnitude. 16, and succeeded in discovering Pluto in 1930. In addition, Tombaugh searched 1,530 square degrees (deg^2) of sky along the ecliptic to a limiting V magnitude of 17.5. No outer solar system objects other than Pluto were found. Luu and Jewitt (1988) searched 200 deg^2 photographically y with a Schmidt telescope to a limit of V = ?0, and 0,34 deg^2 with a CCD camera to R = 24 (V = ?.4.5), both with negative results. 1 evison and Duncan (1990) searched 4.9 deg^2 using a CCD to V = 22.5, again with negative results. Other negative. searches include Cochran et al. (1991) and Tyson et al. (1992.).

Kowal (1989) searched 6,400 deg^2 photographically to V = ?0, discovering the first outer solar system, planet- crossing object (other than PI uto and recogn i zed comets), 2060 Chiron in 1977. Chiron is Saturn-crossing with a perihelion of 8.47 AU and an aphelion of 19.03 AU, just inside the orbit of Uranus. Five additional outer solar system, plane.t-crossing objects have since been discovered; orbital data and estimated radii for all six objects are given in '1'able 1. All of these objects are in chaotic, unstable orbits, with Pholus, 1993 HA_2, and 199S GO having aphel ia beyond Neptune (thus, they pass through the trans-Neptunian region), and with d ynamical lifetimes of 1 0^6 to 108 years (Wetherill 197S; Dones et al. 1995). The maximum inclination among the four objects is 24.7° for 5145 Pholus, suggesti ng that their source reservoi r is likely in the ecliptic plane. The most likely source. is the Kuiper belt region beyond Neptune..

The first successful detection of an object beyond the orbit of Neptune (other than Pluto

and Charon) was by Jewitt and Luu (1992, 1993a). Using a CCD camera on the 2.2 meter University of Hawaii telescope, they searched ~ 1 deg^2 to R = 24.S and found object 1992 QB_1 in August 1992. 1992 QB_1 was at a heliocentric distance of 41.2 AU. The object was magnitude R = 22,8, reddish in color with V - R = 0,7 ± 0.2, and stellar in appearance with no evidence of cometary coma, If the object has a typical cometary albedo of 0.04, then it has a radius of ~130 km. Subsequent observations allowed Marsden (1993a) to determine an orbit for 1992 QB_1 with semimajor axis of 43.8 AU, eccentricity of 0.088, inclination of 2.2°, and orbital period of 290 years. The perihelion distance of 40.0 AU is well beyond the orbit of Neptune.; the aphelion of 47.7 AU is about 2 AU inside the. aphelion distance of Pluto. Dynamical investigations (Duncan et al. 1995; see Section 4) suggest that orbits like that of 1992 QB_1 are stable over the age of the solar system.

The second discovery of a trans-Neptunian object, designated 1993 FW, was by Luu and Jewitt (1993a) who found the R = 22.8 magnitude object at 42.1 All. The discovery image is shown in Figure 1. 1993 FW is similar in size to 1992 QB_1 (possibly slightly larger) but less red in color with V - R = 0.4 ± O. 1, and again, stellar in appearance. A subsequent orbit solution by Marsden (1993b) found a = 43.9 AU, e = 0.041, i = 7.7°, and P = 291 years. Again, this orbit would be expected to be stable. over the age of the solar system,

The next four objects discovered were significantly different in that their heliocentric distances were substantially closer to Neptune., in a region where the orbits cannot be stable. unless protected by some dynamical mechanism, The four objects: 1993 RO (Jewitt and 1.UU 1993b), 1993 RP (Luu anti Jewitt 1993b), 1993 SB and 1993 SC (Williams et al. 1993) were found at heliocentric distances ranging from 32.3 to 35.4 AU. Interestingly, all four objects were approximately 60° from Neptune in the sky, suggesting a possible Trojan-type (1:1 resonance) dynamical relationship. However, Marsden (1994) has preferred an orbit solution for all four objects as being in a 2:3 mean motion resonance with Neptune, similar to the motion of Pluto. Recent orbit solutions (Marsden 1995; personal communication) for all these objects but 1993 RP (for which there are insufficient observations) show that they are in the 2:3 resonance.

Continued searches have now discovered a total of 28 trans-Neptunian objects, which are listed in '1'able 2, in order of discovery. The columns in the. table are the heliocentric distance at discovery, the semimajor axis and eccentricity (if a suitable. orbit solution exists), the orbital

inclination, the orbital period, the R magnitude at discovery, and an estimated radius, based on an assumed cometary albedo of 0.04. Nine of the discovered objects are at heliocentric distances where they might make close approaches to Neptune, unless protected by some dynamical mechanism. The other 19 objects are well beyond the. orbit of Neptune, though the eccentricity of their orbits are only well determined in a few cases so far. Some of these latter objects are in mean motion resonances with Neptune, with high orbital eccentricities.

For the Kuiper belt objects where the orbits are poorly determined, Marsden (1994, 1995, personal communication) has assumed circular orbits for objects beyond 40 AU, and orbits locked in mean motion resonances inside of 40 All. However, it is entirely possible (though not likely) that one or more of these objects are not residents of the Kuiper belt, but rather are Oort cloud comets transiting the region. I'bus, additional astrometric observations are. of extreme importance in determining accurate orbits for all these objects.

The largest objects appear to be 1994 VK_8 and 1995 DC_2 with radii of ~ 180 km (though the size of 199S DC_2 is uncertain), with 1995 KJ_1 somewhat smaller at -160 km radius (assuming an albedo of 0.04). The smallest is 1993 RP at -50 km. The cumulative absolute magnitude distribution of the. 28 objects is shown in Figure 2. 'J 'he very steep slope of the distribution between absolute R magnitude 6.0 and 7.0 is much greater than that observed for the collision all y evolved main asteroid bel t, The steep slope may be. indicative of an upper size limit in the growth of bodies by accretion in the. Kuiper belt, However, given the small number of bodies discovered at this time, this cannot be considered a very robust conclusion. The low slope of the distribution at radii less than ~ 120 km (absolute. magnitudes > 7.0) is indicative of observational incompleteness at the fainter magnitudes.

in addition to large objects, Cochran et al. (1995) have. discovered approximately 30 objects in the Kuiper belt with V magnitudes between 2."/.6 and 28.1 (radii between 6 and 12 km assuming an albedo of 0.04) using deep HST WFPC2 images obtained in the ecliptic. The HST data consisted of 34 WFPC2 exposures of -10 minutes each of a single field obtained on a number of consecutive orbits. Cochran et al.'s data reduction procedure consisted of cleaning the images of fixed objects which are outside the solar system and then stacking the images using drift rates representative of various Kuiper belt orbits. The resulting images were then searched by an automated program for candidate objects. For every real Kuiper belt orbit studied, Cochran et al. also studied an unrealistic orbit to act as a control,

Although at the time Cochran et al, wrote their paper, they had only searched about one-quarter of all reasonable orbits, they found a total of 53 candidate objects in the real-orbit images while only finding 24 in the control images. A chi-square test indicates that there is less than a 1 % chance that these two samples are drawn from the same parent population. Therefore, at the 99% confidence level, they have detected real objects.

Cochran et al. (1995) found that the 2.9 excess objects discovered in the real-orbit images lie in the plane of the ecliptic with inclinations less than ~ 1S'. The inclination distribution is consistent with that found for larger known Kuiper belt objects, thus adding credence to the identification of these objects as Kuiper belt members. In addition, although it is not possible to determine the orbits of these objects with any precision, they had drift rates with respect to the stellar background that are consistent with objects in the 2:3 mean motion resonance with Neptune, with eccentricities between 0.1 and 0.3.

3. Oort Cloud Comets Passing Through the Trans-Neptunian Region

lxmg-period comets from the Oort cloud (Oort 1950; Weissman 1991) which enter the planetary system must pass through the trans-Neptunian region, and thus, can interact with Pluto and Charon. lxmg-period comets are perturbed into the planetary region by a combination of stellar and galactic perturbations. These perturbations tend to randomize the angular momentum vectors of comets in the Oort cloud, leading to a random distribution of orbital inclinations and orientations over the celestial sphere, and a uniform perihelion distribution in the planetary region, as a function of heliocentric distance. The latter was demonstrated with Monte Carlo simulations by Weissman (1977) and analytically by Hills (198 1) who showed that for a randomized distribution

$$f = 2q/a\,(1 - q/2a) \approx 2q/a \quad \text{for } q \ll a \qquad (1)$$

where f is the fraction of the comet population with semimajor axis, a, that has perihelion distance < q, and q is the perihelion distance.. Given an Oort cloud population of 10'2 comets (Weissman 199 1) and a typical semi major axis of 2.2. x 1@ AU (Marsden et al. 1973), equation (1) predicts a uniform perihelion distribution in the planetary region of 28 dynamically new comets per AU per year.

However, the planetary region acts as a sink for long-period comets, with Jupiter (and to a lesser extent Saturn) ejecting them from the solar system on hyperbolic orbits after relatively few returns, typically 5 for Jupiter-crossing comets (Weissman 1979). Jupiter and Saturn act as a barrier to the diffusion of long-period comet perihelia into the terrestrial planets region. Conversely, the cometary flux in the outer planets region is much higher than one would estimate from the observed flux at the Earth. The perihelion distribution for long-period comets from the Oort cloud has been estimated bylkmuhdez(1982) and Weissman (1985); an example is shown in Figure 3. Using this figure, along with Everhart's (1967) estimate that ~ 10 long-period comets with radii ≥ 1 km pass within 1 AU of the Sun per year (most are missed due to observational selection effects), one can obtain a rough estimate, of the long-period comet flux in the trans-Neptunian region.

This was done by Weissman and Stern (1994), who estimated cratering rates on Pluto and Charon due to long-period comets passing through the region. They found that because of the very small cross-sections of Pluto and Charon and their large distance from the Sun, expected cratering rates were extremely low. Even when enhancements in the flux due to random cometary showers from close stellar passages and encounters with giant molecular clouds were included, Weissman and Stern estimated a total cratering rate of only 2.4×10^{-10} yr^{-1} on Pluto, and 7.0×10^{-11} yr^{-1} on Charon. These are equivalent to only one or two impacts on each body over the age. of the solar system. The rms encounter velocity of the comets was 8.2 km/s for either body.

Oort (1950) argued that the cometary cloud surrounding the solar system would be unpopulated at semimajor axes less than $\sim 10^4$ AU because at those distances stellar perturbations on the comet orbits were not sufficient to detach their perihelia from Neptune's influence, However, By] (1983) and Heisler and Tremaine (19S6) recognized that the tidal perturbation from the galactic disk was also significant in perturbing Oort cloud comets, Duncan et al. (1987) showed that the galactic tide could raise the perihelia of comets with semi major axes as small as 3×10^3 AU out of the Uranus-Neptune zone. As a result, they showed that the populating of a massive inner Oort cloud with a population about five times that of the outer, classical Oort cloud, was a natural consequence of the ejection of icy planetesimals from the Uranus-Neptune zone.

Unfortunately, Duncan et al. (1987) remains the only definitive paper on the structure

of the inner Oort cloud, and did not address the perihelion distribution of comets in the inner cloud. That perihelion distribution almost certainly extends into the trans-Ncptunian region. Using equation (1), we can crude] y estimate the flux of comets in the trans-Neptunian region. Assuming a population of 5 x 10^{12} comets and a typical semimajor axis of 3 x 10^3 AU, the density of perihelia is 3.3 x 109 AU^{-1} in the Pluto-Charon region. Because that semi major axis corresponds to an orbital period of 1.6 x 105 years, the flux versus time is -2.0 x 10^4 AU^{-1} yr^{-1}.

The actual perihelion distribution in the trans-Neptunian region is likely a function of heliocentric distance, but much steeper than that determined for the long-period comets in the planetary region as shown in Figure 3. Everhart (1968) showed that planetary perturbations on near-parabolic orbits are relatively insignificant beyond -1.5 times the planet's semimajor axis. On the other hand, the galactic tide is not capable of driving inner Oort cloud cornets to perihelia very far within the orbit of Neptune. Thus, the perihelion distribution of the inner cloud comets is constrained to rise very steeply between 30 and 45 AU.

The inclination distribution of the inner Oort cloud comets is also poorly determined. Duncan et al. (1987) showed that the inner cloud was large] y randomized in inclination by galactic and stellar perturbations at semi major axes > 6 x 10^3 AU. However, inside that distance (which includes the bulk of the inner oort cloud population) the orbits have not been totally randomized, and retain some memory of their ecliptic plane origin.

Given these large uncertainties in orbital distributions, it is difficult to make quantitative estimates of the actual flux of inner Oort cloud comets interacting with Pluto and Charon, Weissman and Stern (1994) did make some crude estimates, They showed that the impact probability and encounter velocity for inner Oort cloud cornets on Pluto and Charon was essentially constant versus the perihelion distances of the comets, and thus was only a function of the total flux of comets crossing Pluto's orbit, and not the detailed shape of the perihelion distribution of those comets. They also showed that because the inner Oort cloud comets are in near--parabolic orbits, their mean impact probabilities and encounter velocities are similar to those determined for long-period comets from the outer Oort cloud. A weakness in Weissman and Stern's analysis is that they assumed random inclinations for the inner Oort cloud comets. The effect of this assumption is to under-estimate the mean impact probability y and over-estimate the mean encounter velocity for those comets,

Because of the much greater density of perihelia of nner Oort cloud comets in the trans-

Neptunian region, Weissman and Stern found that impact rates for inner Oort cloud comets on Pluto and Charon were not negligible over the history of the solar system. Assuming an inner Oort cloud population of 5 x 10^{12} comets, they estimated impact rates of 1.2 x 10^{-8} yr^{-1} for Pluto, and 3.1 x 10^{-9} yr^{-1} for Charon. This translates to 55 and 14 impacts on Pluto and Charon, respective] y, over the history of the solar system, At the mean encounter velocity of 8,2 km See-l, typical comets with nucleus radii of ~ 1.5 km would create craters -15 to 20 km in diameter on Pluto and Charon.

The estimates above for both the inner and outer Oort cloud comets are based on the assumption that the current flux of comets into the planetary region is representative of the mean flux. However, temporal variations in the flux are possible. Random passing stars will on occasion penetrate the Oort cloud and cause massive showers of comets into the planetary region (Hills 1981; Weissman 1995b). The solar system's oscillatory motion perpendicular to the galactic plane carries it into less dense regions of the galactic disk with a corresponding decrease in the galactic tidal force (Matese et al. 1995). Both of these effects will cause temporal variations in the flux of cornets into the planetary system.

Hills (1981) suggested that stars passing through the Oort cloud could initiate showers of comets into the planetary region, particularly if the Oort cloud had a dense inner core, the inner Oort cloud described above. The effect of the sta r passage is to perturb so many comets in perihelia that the comets fill the loss cone, the region in velocity phase space where the comet orbits have perihelia in the planetary region. In effect, the inner planetary region is flooded with comets, and the perihelion distribution shown in Figure 3 becomes uniform with heliocentric distance, at the value dictated by equation (l).

Hut et al. (1987) and Fernández and lp (1987) modeled the dynamical evolution of cometary showers. They showed that the most intense showers could raise the cometary flux at the Earth's orbit by a factor of up to 300. Such showers would be caused by stars penetrating the Oort cloud to -3 x 10^3 AU, which would only be expected to occur about once every 5 x 108 years. More modest showers might occur from star passages at 10^4 AU, which would occur every 5 x 107 years 'l'he duration of a shower is about 2 to 3 x 1@ years.

Weissman (1990) estimated that cometary showers raised the total integrated flux at the Earth's orbit by about a factor of three over the history of the solar system, assuming that the. solar system is currently not in a cometary shower. Fernández (1994) suggested that the fact

that the signature of the galactic tide, i.e., the deficit of dynamically new long-period comets with aphelion directions towards galactic latitudes of 0° and ± 90° as pointed out by Delsemme and Patmiou (1986), is observable in the distribution of long-period comet orbits, is evidence that the solar system is not currentl y experiencing a cometary shower. Weissman (1 994) reached the same conclusion based on the 1/N distribution for the long-period comets, which shows no evidence of a recent stellar perturbation of the inner Oor t cloud. Because of Pluto and Charon's greater distance from the Sun, Weissman and Stern (1994) estimated that showers only resulted in a doubling of the integrated cometary flux at their orbit.

Matese et al. (1995) estimated a factor of four variation in the cometary flux due to the solar system's harmonic motion above and below the. galactic plane, which currently carries the planetary system -75 parsecs out of the galactic plane. However, Matese et al.'s dynamical model did not include stellar perturbations. It is possible that stellar perturbations act to mitigate the variation in the galactic tidal perturbations. At present the solar system has just passed through the galactic plane in the last few million years, so the current steady-state flux is likely at a local maximum.

At present the lack of more detailed dynamical models for the inner and outer Oort clouds make it impossible to significantly improve on the estimates above, Clearly, this is a ripe area for future dynamical studies.

4, The Long-Term Stability of Orbits in the Trans-Neptunian Region

The first detailed study of the stability of orbits in the Kuiper belt was by Torbett (1989) and Torbett and Smoluchowski (1990), who showed that low inclination orbits beyond Neptune are chaotic with Lyapunov times less than 1@ years if their perihelion distances are between 30 and 45 AU. Gladman and Duncan (1990) integrated a modest number of particles initially on circular orbits between 30 and 40 AU for 2×10^7 years and showed that objects with $a \leq 34$ AU would become planet-crossers and thus leave the Kuiper belt. These integrations were modest by current standards. Moreover, Torbett and Smoluchowski assumed fixed orbits for the major planets.

Study of the dynamical evolution of orbits in the outer planetary region over longer

periods has recently been made possible as a result of improved integration codes developed to study the problem (Wisdom and Holman 1991; Saha and Tremaine 1993; Levi son and Duncan 1994), and the availability of high-speed, low-cost computer workstations which can be dedicated for periods of weeks or months to a single dynamical investigation, Since the initial studies noted above, numerical integrations of orbits in the Kuiper belt have been greatly expanded. Levi son and Duncan (1993) and Holman and Wisdom (1993) performed integrations for 10^9 and 2×10^8 years, respectively. In both papers, the authors studied the behavior of objects initially on low-inclination, nearly-circular orbits inside of 45 AU.

The most complete study of the long-term behavior of objects in the Kuiper belt has been performed by Duncan et al. (1995). The authors perfo rmed two sets of numerical integrations. In the first they followed the orbital evolution of 1,300 test particles on initial orbits with low to moderate eccentricity and low inclination within the Kuiper belt over a period of 4×10^9 years, essential y the age of the solar system. In the second, they followed the evolution of 3,000 particles with initially low to moderate eccentricity and moderate inclinations within the Kuiper belt for a period of 10^9 years. Each particle was followed until it suffered a close encounter with Neptune. Once comets can encounter Neptune, they will rapidly evolve (- 10^7-108 years) into the inner planets region, or be ejected to the Oort cloud or to interstellar space.

The results of Duncan et al,'s (1995) 4×10^9 year integrations are shown in Figure 4. The color-cd strips indicate the length of time required for a particle to become a Neptune-crosser as a function of its initial semimajor axis and eccentricity. The initial inclination was 1° for all the particles. Strips that are colored yellow represent objects that survive for the length of the integration, 4×10^9 years. As can be seen in the figure, the Kuiper belt has a complex structure, although the general trends are easily explained. Objects with perihelion distances less than -35 AU (shown as a red curve) are unstable, unless they are near, and presumably librating about, a mean motion resonance with Neptune. Indeed, the results in Figure 4 show that many of the Neptunian mean motion resonances (shown in blue) are stable for the age of the solar system, Objects 'with semimajor axes between ~ 40 and 42 AU are unstable. This is presumably due to the presence of three overlapping secular resonances that occur in this region of the solar system: two with Neptune and one with Uranus (Knežević et al. 1991).

Indeed, secular resonances appear to play a critical role in ejecting particles from the

Kuiper belt. This can be seen in Figure S, which shows some of the results of Duncan et al.'s (1995) 10^9 year integration. Here, the color strips show the length of time required for a particle to become a Neptune-crosser as a function of its initial semimajor axis and inclination. These particles all had initial eccentricities of 0.01. Also shown are the locations of the Neptune longitude of perihelion secular resonances (in red) and the Neptune longitude of the ascending node secular resonances (in yellow) as determined by Knežević et al. (1991). It is important to note that much of the clearing of the Kuiper belt occurs where these two resonances overlap. This includes the low inclination region between 40 and 42 AU. The Neptune mean motion resonances are also shown (in green).

As we mentioned above, the low order Neptune mean motion resonances are stable for low inclinations. However, it can be seen in Figure 5 that these resonances are often unstable for high inclinations. This instability is again most likely due to secular resonances. Figure 5 shows that the secular resonances associated with the longitude of perihelion, as calculated by Knežević et al, (1991), converge on the 3:4 and 2:3 mean motion resonances for large inclinations (although as they pointed out, their theory may have difficulties very near the mean motion resonances and at inclination above - 300). Duncan et al. (1995) show that the unstable orbits in these regions of phase space are chaotic and temporarily librate about both the local mean motion resonance and the nearby secular resonance, confirming that the resonance overlap is the cause of the instability.

Much of the behavior observed by Duncan et al. (1995) has been explained using analytic methods in a recent paper by Morbidelli et al. (1995). Perhaps their most interesting result is an explanations for the stability of the mean motion resonances, particularly those of order 1 (i.e., n:n+1). In the asteroid belt, the mean motion resonances are unstable and are the locations of the Kirkwood gaps. Morbidelli and Moons (1993) and Moons and Morbidelli (1995) have shown that the Kirkwood gaps exist because these mean motion resonances have overlapping secular resonances embedded in them, which cause them to be chaotic. In the Kuiper belt, Morbidelli et al. (1995) show that the 5:6, 4:5, and 3:4 mean motion resonances are free of internal secular resonances, and thus are. stable (at least for low inclinations).

The 2:3 resonance is more complex because it contains the ν_{18} and Kozai resonances (Morbidelli et al. 1995). The ν_{18} is a secular resonance between the precession of Neptune's longitude of the ascending node and that of the. test particle. The Kozai resonance couples the

evolution of a particle's inclination, eccentricity and argument of perihelion. Objects in this resonance have arguments of perihelion that librate. Pluto is such an object (see chapter by Malhotra and Williams in this book). Figure 6 shows the location of these resonances as a function of eccentricity and inclination in the 2:3 mean motion resonance, The location of the known Kuiper belt objects that are in the 2:3 mean motion resonance are also plotted in the figure. These objects are well separated from the secular resonances, which could help to explain their stability.

Finally, it is interesting to compare. Duncan et al.'s (1995) results to the current best orbital elements of the known Kuiper belt objects as determined by Marsden (see Table 2). This comparison is made in Figure 4, The locations of all the Kuiper belt objects with established orbits are shown as filled green circles in the figure. The main result of this comparison is that objects inside of -42 AU have sufficiently high eccentricities that they must be in Neptune mean motion resonances to be stable. Objects outside of this region appear to have lower eccentricities and are not in obvious mean motion resonances (though there does appear to be a cluster of objects around the 4:7 resonance at 43.7 AU). It is interesting to note that this transition occurs near the location of the secular resonances at 40-42 AU.

Looking at Figure 4, it is surprising that there are, as yet, no known objects with semimajor axes between 36 and 39 AU, despite the fact that the simulations indicate that most objects in this region are stable provided their initial eccentricities are less than $\leq 0{,}05$, Only object 1995 GA7 which is currently at 37.9 AU from the Sun, and possibly 1995 GJ at 39 AU, can have their semi major axes in this region of the solar system. Unfortunately, both were just recent] y discovered and more observations are necessary to determine their orbits. If the 36-39 AU, region is indeed not populated, then some mechanism other than the long-term gravitational effects of the planets in their current configuration is likely required to have cleared it. Two mechanisms that may have accomplished this come to mind:

- The hypothetical early outward migration of Neptune would cause its mean motion resonances to sweep through this region thereby sweeping most objects into the mean motion resonances (Malhotra 1995). This mechanism was first proposed to explain Pluto's current orbit (Malhotra 1993). One possible problem with this mechanism is that in order to pump Pluto's eccentricity to its current value, Neptune must have had an initial sernimajor axis of 25 AU, Thus, the initial location of the 1:2 mean motion resonance would have to have been at 40 AU,

inside the location of all the known Kuiper belt objects that are currently not in mean motion resonances (roughly half of the total number). In the context of this mechanism, it is difficult to understand why most of those objects were not captured into the 1:2 resonance as Neptune migrated to its current location. In general, this mechanism predicts that the mean motion resonances would be over-populated relative to a more uniform initial distribution,

• Some process may have pumped up the eccentricity and inclination of particles in this region above e $\simeq$ 0.05 and/or i $\simeq$ 10° where the dynamical lifetimes are short, One method for exciting random motion in a disk is by mutual gravitational encounters between objects in the disk. In this vein, it is interesting to note that the escape velocity of the largest known Kuiper belt object is approximately 200 m/s (assuming a density of 2 g cm^{-3}), which is about 5% of its heliocentric orbital velocity. Thus, if there were initially enough of these objects for the Kuiper belt to be dynamically relaxed by mutual gravitational scattering, then they would have a typical eccentricity of a few percent, not quite enough to depopulate the region of interest. However, there are other mechanisms that could produce. higher eccentricities. For example, if the Kuiper belt initially had objects the size of Charon (R $\simeq$ 600 km), then the typical eccentricity would be $\geq$ 0,1. Indeed, there are arguments suggesting such a population in the past (Stern 1991). In this way, the region of interest may have been depopulated, except in the resonances where large eccentricity orbits are stable. Unlike the previous hypothesis, this mechanism predicts that the mean motion resonances would *not* be over-populated relative to a more uniform initial distribution.

These two explanations are not exhaustive. Physical collisions and gas drag may have played an important role (Stern 1995a). Nonetheless, these two models make very different predictions about the distribution of objects in the Kuiper belt. Thus it seems likely that further observations will help resolve if either mechanism is playing an important role.

5. The Number of Kuiper Belt Objects and Their Total Mass

There are several independent methods for estimating or constraining the total mass and/or total number of objects in the Kuiper belt. These include: 1) mass constraints from the gravitational effects of the Kuiper belt on the heliocentric orbits of objects in the solar system,

2) number constraints from the effects of the Kuiper belt on the Pluto-Charon binary orbit, 3) number constraints from telescopic searches for Kuiper belt objects, and 4) number estimates of small objects from the requirement that the Kuiper belt be the source of the Jupiter-family comets. Each of these are addressed below.

The first estimate of the mass of the Kuiper belt was performed by Whipple (1964), who examined the possible perturbative effects of a. distant comet belt on the orbit of Neptune. He concluded that a comet belt totaling -10 $M_\oplus$ at 40 AU, or -20 $M_\oplus$ at 50 AU, could better explain the apparent discrepancies in Neptune's motion, than assuming a significant mass for Pluto. It is now recognized that the discrepancies in Neptune's motion are not real (Standish 1993), but that was not known in 1964.

Whipple's work led Hamid et al. (1968) to study the motion of seven short-period comets with large aphelion distances, in particular comet P/Halley. They concluded that the mass of the trans-Neptunian comet belt could not exceed 0.5 $M_\oplus$ if the belt was at 40 AU, and 1,3 $M_\oplus$ if it was at 50 AU. Similar results were obtained by Yeomans (1986) in his study of the motion of cornet Halley. Hogg et al. (1991) simulated the perturbations on comet Halley by a hypothetical comet belt beyond Neptune, and then estimated what minimum mass might be detected with modern observations. Although they claimed a much tighter upper limit on the Kuiper belt mass than Hamid et al., their result was based on incorrect assumptions about the positional accuracy obtainable with current astrometric observations. In reality their limit is no better than those found by Hamid et al. (1968) and Yeomans (1986).

Most recently, Anderson et al. (1995) used Pioneer and Voyager spacecraft tracking to set an upper limit of -0.7 $\pm$ 0.6 $M_\oplus$ of unseen matter interior to the orbit of Neptune, and less than "a few" $M_\oplus$ in the Kuiper belt located 10 AU beyond Neptune. Anderson et al. suggest that the negative sign of the upper limit may be indicative of a non-symmetric mass distribution beyond Neptune's orbit. Thus, it will be very interesting to see what additional results are obtained from tracking of these spacecraft as they proceed through the Kuiper belt region. The Voyager 1 and 2, and Pioneer 10 and 11 spacecraft are currently at heliocentric distances between $\sim$38 and 60 AU, ranging from the inner edge of the dynamically active Kuiper belt to the dynamically stable region, well beyond Pluto's orbit. The Voyager 1 and 2 spacecraft could conceivably operate until about the year 2018, when they would be at heliocentric distances of 139 and 116 AU, respectively.

In summary, the Kuiper belt has not been unambiguously detected by any study of its gravitational effects on heliocentric orbits of solar system objects. These studies have only been able to place upper limits on its mass, the best being $M_{KB} \leq 0.5\ M_{\oplus}$ if the belt is at 40 AU, and $\leq 1.3\ M_{\oplus}$ if it is at 50 AU.

Weissman et al. (1989) attempted to use the very low eccentricity y of the orbit of Pluto's satellite Charon, then thought to be -104, to set an upper limit on the impact rate of comets on Pluto and Charon, and thus an upper limit on the population and mass of the Kuiper belt, However, the limit they found, -15 $M_{\oplus}$, was not as sensitive as those described above.

More recently, Tholen and Buie (1995) have reported astrometric evidence for a significant orbital eccentricity for Charon, with a likely value near e = 0.003. This eccentricity is surprising] y large because the tidal spin-down time of the Pluto- Charon binary is short, -9 x 10^6 years, compared to the age of the solar system (Weissman et al. 1989). Levi son and Stern (1995) have placed crude estimates on the total number of large objects in the Kuiper belt by studying the perturbations by these objects on the binary orbit of Pluto and Charon. They show that Kuiper belt objects passing between Pluto and Charon can excite the eccentricity of that orbit. Under the assumption that this mechanism is the only one of importance, Levison and Stern's preliminary results suggest that there are between 3 x 1@ and 3 x 108 (with a preferred value of 3 x 10^7) Kuiper belt objects with radii between 20 and 330 km within 50 AU of the Sun. Since other unrecognized mechanisms may also be important, this estimate should be viewed as an upper limit.

The searches that discovered the Kuiper belt objects listed in Table 2 can also be used to estimate the total number of objects in the Kuiper belt. In order to accomplish this, a consistent set of observations is required. Jewitt and Luu (1995) performed such an analysis on the 7 objects that they discovered in their Mauna Kea survey, which covered 1.2 deg^2 of sky. They found that there are -6 objects per square degree brighter than their limiting magnitude, $m_R \simeq 24{,}5$. All of their discovered objects had radii, $R \geq 50$ km and heliocentric distances, r, between 30 and 50 AU. In addition, the largest inclination in their study was i = 8". Combining these numbers they concluded that there must be - 3,5x 1@ objects with $R \geq 50$ km at $30 < r \leq 50$ AU from the Sun. Since Kuiper belt objects have now been found in orbits inclined up to 22°, Jewitt and Luu's estimate is likely only a lower limit, If each of the 3.5 x 10^4 objects has a radius of 50 km with a density of 1.0 g cm^{-3}, then the minimum mass of the

Kuiper belt is -1.8 x 10^{25} g, or -0.003 $M_{\oplus}$, Jewitt and Luu (1995) also noted that past observational searches, in particular Kowal (1989), set an upper diameter limit of 600 km on comets between 30 and 50 AU.

Similarly, Cochran et al.'s (1995) HST observations can be used to constrain the number of Halley-sized objects in the Kuiper belt. They found 29 objects with V magnitudes between 28.1 and 27.6. Assuming that these objects were in the Kuipcr belt and that their albedo is 0.04, this magnitude range corresponds to radii between 6 and 12 km. Cochran et al.'s observations only covered about 4 square arc minutes of sky. Thus, their observations imply that there are -2 x 10^{8} comets in this size range in the orbits they studied. This value should be viewed as a lower limit, however, since Cochran et al, only searched about one-quarter of the available orbital parameter space.

The total number of comet-sized objects in the Kuiper belt with $1 \leq R \leq 10$ km can be estimated from the observed population of Jupiter-fat nil y comets. Following Duncan et al. (1995), the total number of Jupiter-famil y comets (both active and extinct) is

$$N_{JFC} = N_{KB}\ p_e\ f_{JFC}\ L_{JFC} \quad , \qquad (2)$$

where N_{KB} is the current number of comets in the Kuiper belt, p_e is the mean probability that any comet between 30 and 50 AU will escape the Kuiper belt per year, f_{JFC} is the fraction of those comets that become Jupiter-family comets once they leave the Kuiper belt, and L_{JFC} is the dynamical lifetime of a Jupiter-family comet. By direct numerical integrations of the known Jupiter-family comets, Levison and Duncan (1994) showed that their median dynamical lifetime is 3.3 x 10^{5} years. Duncan et al. (1995) found that p_e = 3 to 5 x 10^{-11} yr^{-1} for objects inside of 50 AU, depending on the assumed eccentricity of Kuiper belt objects; we adopt $p_e = 4 \times 10^{-11}$ yr^{-1}. From numerical integrations of objects once they leave the Kuiper belt, Levison and Duncan (personal communication) found that $f_{JFC} = 0.34$. The total number of Jupiter-family comets can be estimated from the integrations of known comets by Levison and Duncan (1994). The total number of known active Jupiter-family comets with perihelia less than 2.5 AU is approximately 150 (Marsden and Williams 1995 lists 154 known short-period comets with q < 2.5 AU). Levison and Duncan (1994) found that approximately 10% of comets are active and that they spend approximately 7 % of their lifetime with perihelia < 2.5 AU. Thus, $N_{JFC} \simeq 2.1$ x 1 0^{4}. Solving for N_{KB}, one finds that there are $\sim 5 \times 10^{9}$ comets in the Kuiper belt inside of 50 AU. Taking Weissman's (1990) estimate of the average cometary nucleus mass of 3.8 x 10^{16}

g, the total Kuiper belt mass between 30 and 50 AU is $\sim 2 \times 10^{26}$, or 0.03 $M_{\oplus}$.

The largest uncertainties in this estimate lie. with p_e, which is sensitive to the current distribution of comets in the Kuiper belt, and with N_{JFC}, which is a function of the comets' physical lifetime. Each of these are uncertain by a factor of a few. Also, it is likely that not all of the active Jupiter-family comets with perihelia < 2.5 AU have been discovered so far. Thus, the above estimate is likely good to about an order of magnitude.

Duncan et al. (1995) combined this estimate of the number of comets in the Kuiper belt with their 4 x 109 year integrations to produce a model of the current surface number density in the Kuiper belt. The overall result is shown in Figure "/, which gives the radial distribution of comets in the Kuiper belt after 4 x 109 years, Initially, comets were assumed to follow a $1/r^2$ surface density distribution and had an initial eccentricity y of 0.0S. In addition, the model assumes that the only important process that sculpted the Kuiper belt is the gravitational perturbations of the major planets in their current configuration. The model does not take into account the effects of dissipation, collisions, or the possible early radial migration of the planets. It predicts that the trans-Neptunian region is largely depleted at $r \leq 34$ AU, whereas the Kuiper belt population is relatively untouched at r > 45 AU. It also predicts that 38% of the comets originally formed between 34 and 45 AU have survived over the history of the solar system.

However, the discovery statistics for the 28 Kuiper belt objects found so far are problematic. If one take the discoveries at face value, too few comets have been found at distances < 40 AU, as compared with the "eroded" Kuiper belt distribution shown in Figure 7. Also, it is interesting to note that no large objects have been found at distances > 46 AU. A likely explanation for this is that the observers are overestimating the limiting magnitudes of their surveys.

The constraints on the total number of objects in the Kuiper belt are listed in Table 3. In addition to those discussed above, two more have been listed. For large objects, Kowal's (1989) search that discovered Chiron should have found any Pluto-sized objects within 60 AU of the Sun. Thus, there is only one such object within 50 AU, Pluto. For the smallest objects, Stern (1995a) argues that if the Kuiper belt was populated by objects that followed a simple power law size distribution with a slope of -3 (the value found for comets by Shoemaker and Wolfe, 1982), then the system would have evolved due to physical collisions over the age of the solar system, so that objects smaller than -0.5 km would have been destroyed. However, it

should be noted that the exact value of this lower size cutoff is very model dependent, and thus the credibility of this constraint is much less than the others listed in Table 3,

Weissman and Stern (1994) estimated impact rates for Kuiper belt comets on Pluto and Charon. As with the comets in the inner Oort cloud, they found that the mean impact probability and encounter velocity for Kuiper belt comets was only a slowly varying function of perihelion distance. Thus, the largest unknown was in the total number of Kuiper belt comets. Assuming a population of 10^9 comets in circular orbits between 40 and 50 AU with random inclinations between O and 10°, Weissman and Stern found impact probabilities of 5.4 x 10^{-7} and 1.0 x 10^{-7} for Pluto and Charon, respectively. These translate to 2.4 x 10^3 impacts on Pluto and 460 impacts on Charon over the history of the solar system. Mean encounter velocities were 1.6 km See-l for either body. At the mean encounter velocity, typical comets with nucleus radii of -1.5 km would create. craters -6 to 9 km in diameter on Pluto and Charon. Given the total Kuiper belt population estimate of 5 x 109 comets between 30 and 50 AU by Duncan et al. (1995), total expected impacts would be 5 times the numbers given by Weissman and Stern (1994).

6. The Size Distribution of Small Outer Solar System Objects

By culling information from a variety of sources, including both observed comets and Kuiper belt objects, it is possible to attempt to construct an estimate of the size distribution of icy planetesi reals formed in the outer solar system, Much of what follows is crude, and the results are not intended to be a finished product. On the contrary, the results should be viewed as a forum for a comparison of the known theoretical and observational constraints on the sizes of observed long- and short-period comets and Kuiper be] t objects.

The results listed in Table 3 are displayed in Figure 8, which plots the cumulative number of objects between 30 and 50 AU from the Sun larger then radius R, as a function of R. The constraints listed in the table are shown as filled circles in the plot. It is clear that the size distribution is not a simple power law, but has a fairly complex structure.

The most critical number in this discussion is the estimate of the total number of comets in the Kuiper belt (marked 1 in the figure), based on the observed number of short-period

comets with q < 2.5 AU. It is also the most uncertain. As discussed in Section 5, this number can be off by as much as an order of magnitude because of uncertainties in the physical lifetimes of comets and the current orbital element distribution of objects in the Kuiper belt, In addition, the location of this point on the abscissa, which represents the radius of the smallest visible comet, is also unknown. Its value is thought to be near 1 km, but is uncertain by at least a factor of two. These uncertainties are represented by the. dotted blue box in the figure. The uncertainties in the other data points that are not upper or lower limits are less than or about equal to the size of the point.

In addition to the data in Table 3, there are other observational results that constrain the slope of the size distribution. At small sizes, Shoemaker and Wolfe (1982) used photometry of distant cometary nuclei by Rocmer (1965), Roemer and Lloyd (1966), Roemer et al. (1966), and cratering on the Galilean satellites to estimate the size distribution of comets. They concluded that comets follow a differential size distribution power law, $n(R)\,dn \propto R^{-q}\,dR$, with a slope of $q = 3$ for comet sized objects, $1 \leq R \leq 10$ km. If it is assumed that this power law is valid for all sizes in the Oort cloud and the Kuipcr belt, and that there are 5 x 1@ comet sized objects in the Kuiper belt (see Section 5), then the resulting integrated size distribution is represented by the blue line marked 'A' in Figure 8. However, if this power law is extended to larger objects, it predicts two orders of magnitude more 50 km objects than are observed. This suggests that the slope of the power law must be much steeper at larger sizes. Note that the heavy solid line overlapping this power law indicates the range of sizes for which this power law has been proposed,

Rahe et al. (1995) pointed out several problems with Shoemaker and Wolfe's (1982) size distribution, in particular the fact that they had to assume that on average, 88% of the light of the cometary nuclei observed by Roemer and colleagues was due to unresolved coma, in order to make their size estimates match their cratering rate estimates for the Earth. Roemer's observations were fairly primitive as compared with modern observing techniques and it has been repeatedly shown (Jewitt 1991) that comets often display coma far beyond the distances at which Rocmer and colleagues made their measurements. Thus, both the size estimates and the slope of the size distribution determined by Shoemaker and Wolfe (1982) is open to question.

Cochran et al, (1995) used their HST WFPC2 observations to constrain the slope of the size distribution of objects with radii between 6 and 12 km. Although they had to severely

massage their data and assumed that the objects were in the 2:3 mean motion resonance to determine their distances, they found that $3 \leq q \leq 5$. The q =3 and the q =5 power laws are plotted in Figure 8 in green and are marked with the letters 'B' and 'C', respectively, Again, the heavy solid lines overlapping these power laws indicate the range of sizes for which they have been determined.

At larger sizes, the q= 5 slope ('C') appears to give good agreement with the estimate of the Kuiper belt population by Jewitt and Luu (1995) for objects with $R \geq 50$ km, and the existence of only one Pluto-sized object between 30 and 50 AU. However, unless the size distribution is unusually complex, this means that the population estimate by Levi son and Stern (1995) based on perturbations of Charon's orbit is indeed an upper limit, with a true value perhaps two orders of magnitude less than Levi son and Stern's estimate.

An additional problem is with regard to the slope of the size distribution for the large Kuiper belt objects found by Jewitt and LUU (1995). They used a Monte Carlo technique to simulate the discovery of objects in a Kuiper belt with a surface density that falls as $1/r^2$ outside of 32 AU. Jewitt and Luu assumed that the size distribution of these objects follows a power law, truncated at an upper size limit of R = 200 km. They found that $1 \leq q \leq 2$ for the seven objects discovered in their Mauna Kea survey ($50 < R < 200$ km).

We have duplicated the Monte Carlo simulations by Jewitt and Luu (1995), adding in a more detailed model of the dynamical erosion of the Kuiper belt, and experimenting with different size distributions for the bodies and limiting magnitudes for the searches. The results of these studies will be published elsewhere but we can outline some of our preliminary conclusions here:

- The true limiting magnitude at which the current Kuiper belt searches are complete is $m_R \simeq 23.0 \pm 0.3$, with the searches by Jewitt and colleagues being somewhat better than the others. Jewitt and colleagues have found 4 of the 5 objects fainter than $m_R = 23$, but we do not see evidence that their searches are complete to $m_R = 24.5$ as they claim.

- The size distribution of the 28 objects can best be fit by a power law distribution with $q \simeq 2 \pm 1$, a somewhat broader range than that found by Jewitt and Luu. An even steeper power law could be made to fit the data if the limiting magnitude of the searches was brighter than the value of 23.0 we conclude above, Given the limited statistics of the searches, we can not rule out this possibility, although the fit to the. Monte Carlo mode] results would not be as

good.

Thus, the available data seems to indicate that the size distribution of the known objects in the Kuiper belt at R > 50 km is not as steep as q = 5. The red lines in Figure 8 show two power laws with q =2 (marked 'D') and q=' 1 (marked 'E') under the assumption that there are 3.5 x 10^4 objects with 50 < R < 200 km. However, these flat slopes can only be valid over a very limited size range, as they predict between 10^3 and 1@ Pluto-sized objects at the larger sizes, and at least three orders of magnitude. too few comets at the smaller sizes, Jewitt and Luu (1995) also noticed this and suggested that there is a flattening, or a "shelf' in the size distribution between R = 50 and 200 km.

A comparison between the above power laws and the circles in Figure 8 shows that q =3 fits the constraints fairly well for objects with $R \leq 10$ km. At $R > 10$ km the circles indicate a slope of about q=5. Thus, the size distribution of objects in the Oort cloud and the Kuiper belt might best be described by a broken power law ((Greenberg et al. 1984; Weissrnan 1990; Tremaine 1990) of the form

$$n(R) \propto \begin{cases} 0 & \text{if } R < R_{small} \\ R^{-q1} & \text{if } R_{small} \leq R \leq R_o \\ R^{-q2} & \text{if } R \geq R_o \end{cases}, \qquad (3)$$

where R_{small} is the radius of the smallest object, and R_o is the radius where the power law changes slope, The solid black curve shows such a distribution with $R_{small} = 0.5$ km, $R_0 = 10$ km, $q1 = 3$, and $q2 = 5$.

Broken power laws of this form have been found independently for icy bodies in the outer solar system. Weissman (1990) and Bailey and Stagg (1988) each estimated the differential mass distribution of long-period comets, based on the brightness distribution of long-period comets (with comae), corrected for observational selection effects, found by Everhart (1967). Converting the mass distribution of Weissman (1990) to a size distribution, the slopes are $q1 = 3.2$ at smaller sizes, and $q2 = 5.4$ at R > 6.3 km. Bailey's slopes are somewhat steeper due to a different conversion equation between cometary brightness, H_{10}, and nucleus mass. We note however that these empirical y derived size distributions suffer from some of the same weaknesses as that noted for Shoemaker and Wolfe.'s (1982) work.

Greenberg et al. (1984) found a similar broken power law distribution for cometary bodies accreted in the Uranus-Neptune zone, using a particle-in-a-box type simulation. They

began with a distribution of cometary nuclei with a power law distribution with q= 3.2 between 0.25 and 8 km in radius, with larger bodies forming due to accretion and smaller bodies due to collisions. The break between the two slopes in their size distribution was at a radius of 8 km.

The size distribution described in equation (3) seems to fit the circles and Shoemaker and Wolfe's (1982) power law fairly well. However, it is inconsistent with the slope estimated for 50-200 km objects. If the shelf in the size distribution at -50-200 km is real, then it may hold important clues to the history of the Kuiper belt. It is possible, for example, that the relatively few Kuiper belt objects found so far represent the beginning of a runaway growth of larger objects in the belt.

An example of this type of runaway growth profile can be seen in simulations by Wetherill and Stewart (1993) shown in Figure 9. Note the small "shelf" of runaway objects which develops at large masses, at the lower right in the figure. Although a direct quantitative comparison between these results and the Kuiper belt size distribution is not valid because Wetherill and Stewart (1993) used initial conditions appropriate for the inner solar system, some of the general trends seen in Figure 9 may be valid for all runaway growth situations (Stewart, personal communication). The size distribution of the. smallest objects is determined by fragmentation, thus it should follow a power law with $q \simeq 3$ (Hartmann 1969), This is seen in both Wetherill and Stewart's (1993) calculations and in the Kuiper belt (as suggested for the size distribution of the comets). The size distribution of larger objects is determined by accretion dynamics and should have a steeper slope. Recall, that the size distribution in the Kuiper belt is fit fairly well by a q=5 power law for sizes $R \geq 10$ km.

At some characteristic large size, the runaway growth models predict that there should be a flat shelf (seen at $m \simeq 10^{25}$ g in Figure 9) in the size distribution. A similar runaway shelf is seen in Greenberg et al.'s (1984) size distribution for objects accreted in the Uranus-Neptune zone at radii > 250 km. Finally, the runaway growth models require a very steep slope or cut-off at larger sizes. Again, this is seen in the Kuiper belt by the lack of Pluto-sized objects.

There are problems with this comparison between the Kuiper belt objects and the accretion simulations. Runaway growth typically occurs for only a very small fraction of the objects in the theoretical simulations, typically - 10-1(' of the population as seen in Figure 9. If we interpret the $R \geq 50$ km bodies in the Kuiper belt as the beginnings of a runaway population, then they constitute more than 10^{-6} of the population, In addition, they occur in the

Kuiper belt at smaller masses and radii than that suggested by either the Greenberg et al. (1984) or the Wetherill and Stewart (1993) simulations. This leads us to doubt the interpretation that what we are seeing at R > 50 km is the result of runaway growth. However, it is a ripe area for future study.

Given the limited number of objects which have been discovered in the Kuiper belt to date as well as the varying limits on the area and depth of the individual searches, any conclusions about the size distribution in the belt must be regarded as highly speculative. Nevertheless, the Kuiper belt is clearly a rich area for future studies of the growth of planetesimals in the solar nebula. The discovery of additional objects, along with accurate photometric measurements from which their sizes can be inferred, will hopefully help to shed more light on this problem.

7. Neptune Trojans

Because of its 2:3 resonance with Neptune, Pluto regularly passes through the Neptune Trojan regions when it is near perihelion. In fact, Pluto is currently in Neptune's L_5 region. Although there has been considerable speculation about objects locked in Trojan-type libations with planets other than Jupiter (Everhart 1973; Weissman and Wetherill 1974; Mikkola and Innanen 1992), only one librating object has been identified to date. Surprisingly, asteroid 5261 Eureka was found to be in a 1:1 Trojan resonance with Mars (Bowell 1991; Mikkola et al. 1994).

Recent interest in the possibility of Neptune Trojans was stimulated by the discovery of ~100 km sized objects in the trans-Neptunian region. A surprising aspect of the Kuiper belt objects is that about 40% of the bodies found to date are too close to Neptune's orbit for their orbits to be stable, unless they are in a mean motion resonance with that planet (see Section 4). Early attention was paid to two particular mean motion resonances: the 2:3 resonance and the 1:1 Trojan libations. The existence of Neptune Trojans appears plausible because: 1) Jupiter is known to have a large number of Trojans (Shoemaker and Wolfe 1982); and 2) numerical studies indicate that the Lagrange points of other giant planets may also be stable (Innanen and Mikkola 1992, Holman and Wisdom 1993).

Further observations of the discovered Kuiper belt objects between 30 and 40 AU, coupled with long-term numerical integrations have shown that the majority of them are most likely in the 2:3 resonance, one is most likely in the 3:4 resonance, and three are most likely in the 3:5 mean motion resonance with Neptune (Marsden, private communication; also see Duncan et al. 1995). Marsden has concluded that it is unlikely that any of these objects are Neptune Trojans.

Marsden's conclusion raises the question as to whether Neptune's Trojan regions are currently populated. The first step in answering this question is to determine whether the Trojan regions are dynamically stable. No complete survey of the dynamics of the Neptune Trojan regions is yet available. Only two papers have addressed this topic. Mikkola and Innanen (1992) studied the behavior of 11 test particles initially near the Neptune Trojan points for 2 x 107 years. They placed their particles initially at the L_4 point on near-circular orbits, but uniformly varied the initial semimajor axis between 30.06 AU (which is that of Neptune) and -30.81 AU. They found that only 3 particles were stable for the length of their integration, all of which librated about the 1:1 resonance. The angle between Neptune and the stable test particles as seen from the Sun, ϕ, was constrained to lie between -30' and -110', a maximum libration amplitude of $\sim 80°$.

Holman and Wisdom (1993) performed a 2 x 107 year integration of objects initially in near-circular orbits near the Lagrange points of all the outer planets. The test particles were given the same eccentricity, inclination, mean anomaly, and longitude of the ascending node as each of the Jovian planets. The argument of perihelion was uniformly varied between O and 360°. The initial semimajor axis was varied between 0.96 a_P and 1.04 a_P, where a_P is the scmimajor axis of the planet.

The results of their calculation for the Neptune Trojan regions are shown in Figure 10. Each circle shows the initial semimajor axis and the initial ϕ of an orbit that was stable for the entire integration, 2 x 107 years. One of the more surprising results of Holman and Wisdom's integration is the asymmetry between the L_4 and the 1.5 swarms. Holman and Wisdom studied the Trojan regions of all four Jovian planets and Neptune is the only one to show an asymmetry. It is not yet understood why this asymmetry exists,

Although ambitious for their time, the papers discussed above did not integrate long enough or cover orbital element space well enough to determine whether the Neptune Trojan

regions are stable, and if so, where to look in the sky in order to find its members. Thus, we undertook a more complete survey of the Neptune Trojan regions, where we integrated orbits of hypothetical Neptune Trojans for 4 x 109 years. Our results are presented in terms of the libration amplitude, D, and the proper eccentricity, e_p, as defined by Levison et al. (1995), in order to facilitate comparison with the sear ches for Kuiper belt objects.

We numerically integrated the orbits of 70 massless L_4 Neptune Trojans in three dimensions under the influence of the Sun and the four giant planets in their current orbits. The equations of motion for this system were integrated using the Mixed Variable Symplectic scheme developed by Wisdom and Holman (1991). A. timestep of 1 year was used for the calculation. The simulation lasted for 4 x 10^9 years, the age of the solar system,

The initial positions and velocities for the planets were kindly supplied to us by Myles Standish from JPL Developmental Ephemeris DE-245. Each test particle had a different initial value of D and e_p. The initial proper elements were chosen from a grid of 10 values of e_p ranging from O to 0.2 and seven values of D between 0 and 120°. The test particle orbits were initially in the same plane as Neptune. We were interested in whether an orbit was stable for the length of the integration, We considered an orbit unstable if the particle either suffered a close approach with any of the giant planets or was ejected from the solar system.

The results of the integration are shown in Figure 11, which is a contour plot giving the lifetime of the test particles as a function of their initial proper orbital elements. Contours for 10^6 through 4 x 10^9 years are shown. Notice that the stable region shrinks quite dramatically over this time span. This result is consistent with results for the Jupiter Trojan regions (Levi son et al. 1995). The integration shows that there do exist Neptune Trojan orbits that are stable for the age of the solar system.

Stable Neptune Trojans must have libration amplitudes less than 60° and proper eccentricities less than 0.05. It is interesting to note that this range for D is similar to that Levison et al. (1995) found for the Jupiter Trojans. Although, the similarity may be a coincidence, it may also indicate a fundamental characteristic of the 1:1 Trojan resonance. On the other hand, the maximum stable proper eccentricity, e_p for the Neptune regions is a factor of three smaller than that of the Jupiter regions ($e_p \leq 0.15$ in the Jupiter regions),

As discussed above, Figure 11 shows the results of our integration in terms of the initial proper orbital elements. These proper elements are a crude approximation to constants of the

motion. It is possible to determine the libration amplitude by directly measuring in the integrations ϕ, the range of differences between the mean longitude of the test particles and Neptune, The libration amplitude of our stable test particles range from 40° to 60'. There are no small amplitude librators in this simulation, This result is consistent with those of Holman and Wisdom (1993), They placed a test particle at the L_4 of Neptune and found that it explored a range of ϕ that extended 35°. They offered no explanation for this behavior.

In order to attempt to understand why small D orbits do not exist in our integration, we performed a very short, 2 x 104 years, integration with 500 test particles. All of the test particles were in initially circular orbits in the. orbit pkme of Neptune. We varied their initial mean longitude and semimajor axis. Surprisingly, we found that the semi major axes of these test particles did not librate about that of Neptune's as the analytic theory predicts, Instead, they librated about a point about 0.33 AU farther from the Sun. In this set of simulations, the smallest libration amplitude we found was 4°. This particle had an initial mean longitude that differed from Neptune's by 60" and an initial semimajor axis that was 0.33 AU larger than Neptune's. In addition, we found that this offset is a function of the proper eccentricity. At e_p = 0.15, the offset is 0.37 AU. Why this offset in semimajor axis exists still remains to be determined.

The results of our integrations show that stable orbits over the age of the solar system do exist in the Neptune Trojan regions. However, ground-based searches of the trans-Neptunian region have failed to detect any objects that can be identified as Trojan-type librators (Cochran et al.'s 1995 HST observations did not look in the Neptune Trojan region). We can estimate an upper limit on the total number of Neptune Trojans from these searches. As discussed above, Jewitt and Luu (1995) published the only set of observations where enough detail is presented to make such an analysis. They covered 1.2 square degrees of sky down to a limiting magnitude, $m_R \simeq 25$. Since the heliocentric distance. of Neptune Trojans do not vary very much due to their small eccentricities, that limiting magnitude corresponds to a radius of -25 km, assuming an albedo of 0.04. From our integrations, we can estimate that the Neptune Trojans cover about 120° of the ecliptic. Thus, to a 99% confidence level there must be $< 500\ i_{NT}$ objects larger than 25 km in the Neptune Trojans region, where i_{NT} is the maximum inclination of the Trojan population in degrees, Note that this limit is derived from Jewitt and Luu's (199S) initial survey which discovered one-quarter of the total known Kuiper belt objects, Therefore,

an upper limit based on all the surveys is most likely a factor of a few smaller than the one quoted here.

This population estimate for the Neptune. Trojans can be compared with Jewitt and Luu's (1995) estimate of 3.5 x 10^4 Kuiper belt objects with R $\geq$ 50 km between 30 and 50 AU, assuming a maximum inclination, i_{KB}, of 8°. Stated similarly, the number of Kuiper belt objects with R $\geq$ 50 km is 4.4 x 10^3 i_{KB}. Assuming a modest, q =2 power law for the Kuiper belt size distribution between R = 25 and 50 km (likely an underestimate, see Section 6), this suggests that there are 1.8 x 10^4 i_{KB} objects with radii $\geq$ 25 km, or more than 30 times the upper limit on the population of the Neptune Trojan regions,

This relatively small population for the Neptune Trojan regions could conceivably still result in some hundreds of impacts on Pluto and Charon over the age of the solar system. However, the population ratio of 30 times as many Kuiper belt objects versus Neptune Trojan objects above, is a very conservative estimate and the actual ratio is likely much greater. In addition, the upper limit on the Trojan population is highly conservative since it is based on only a fraction of the telescopic searches made to date. Thus, the net effect of Trojan impacts on Pluto and Charon is likely only a few tens of impacts on Pluto and Charon over the age of the solar system, if that,

8. Discussion

Our understanding of the outer planetary region beyond Neptune has progressed impressively in the past 15 years. For the prior half century, the trans-Neptunian region appeared to be populated only by Pluto and occasional transient long-period comets from the Oort cloud. But Pluto proved to be only the largest end-member of a huge population of comets in the trans-Neptunian region, remnant icy planetesimals from the origin of the solar system, In addition, we now believe that the Oort cloud likely includes a dense inner core of comets which likely extends in to the orbit of Neptune.

In the last five years, research on the trans-Neptunian region has exploded on both observational and theoretical fronts, New telescope technology, including large format CCDs, has allowed searches of large areas of sky to a magnitude of V $\simeq$ 23-24, The Hubble Space

Telescope has allowed discovery of objects at V $\simeq$ 2.8. Advances in numerical integration codes and CPU speed have made it possible to integrate thousands of test particles for the age of the solar system. It is interesting to note that the integrations in Duncan et al. (1995) would have taken between 1,000 and 2,000 CPU years if the technology and codes employed in Duncan et al. (1988) had been used. These advances have. provided the first meaningful understanding of the trans-Neptunian region:

- The Kuiper belt exists. There are -57 known objects that are believed to reside in it, Twelve of these have orbits that are well enough determined to show that they are stable for the age of the solar system.

- The available observations of the Kuipcr belt implies that there are at least 2 x 10^8 objects with radii larger than 6 km and at least 3.5 x 10^4 objects with radii larger than 50 km within 50 AU of the Sun. Theoretical arguments with regard to the origin of Jupiter-family comets suggest that there is a total of -5 x 10^9 objects with R $\geq$ 1 km in this region of the solar system. The total mass of the Kuiper belt within SO AU is on the order of 0.03 -0.1 Earth masses, $M_\oplus$.

- Objects in the trans-Neptunian region follow a complex size distribution. The slope of the size distribution for objects with R $\leq$ 10 km appears to be moderate with a q $\simeq$ 3. For objects larger than 10 km, the slope becomes steeper, having q $\simeq$ 5. It is possible that there is a range of radii between 50 and 200 km where the size distribution becomes relatively flat with q $\simeq$ 2. If this flat region exists, then there must be a very sharp drop in the size distribution for objects with radii larger than -200 km.

- There is a complex structure to the Kuiper belt caused by both mean motion and secular resonances. Overlapping secular resonances induce instabilities in large regions interior to 42 AU, especially at inclinations $\leq$ 25°. Low order mean motion resonances provide a stabilizing protection mechani srn at i $\leq$ 2.5°, but are destabilizing at higher inclinations,

- The discovered objects seem to divide the Kuiper belt into two distinct dynamical zones. Inside of 40 AU, all the objects with well deter mined orbits have eccentricities greater then 0.1 and are trapped in mean motion resonances with Neptune. Objects beyond 40 AU tend to have eccentricities less than 0.1 and are not, in general, in resonances,

As with many scientific endeavors, the discovery of new information tends to raise more questions than it answers. Such is the case here. Even the original argument that suggested the

Kuiper belt is in doubt. Edgeworth's (1949) and Kuiper's (1951) original arguments were based on the idea that is seemed unlike] y that the. disk of planetesimals that formed the planets would have abruptly ended at the current location of the outermost known planet, An extrapolation into the Kuiper belt of the current surface density of nonvolatile material in the outer planetary region predicts that there should be about 30 $M_\oplus$ of material there. However, our best estimates are that there is only about 0,03 -0.1 $M_\oplus$ between 30 and 50 AU.

Were Kuiper and Edgeworth wrong? Is there an edge to the planetary system? Or, did some process or processes remove the excess material? The dynamical effects of the planets in their current configuration clearl y cannot. by themselves be responsible. Stern (1995b) points out that the collision rates bet ween objects in a Kuiper belt much more populous than our own are large, and suggests that collisional erosion played an important role in removing the excess mass. If this is indeed the case then over 99.6% of the mass had to bc removed over the history of the solar system.

The idea of a historically more massive. Kuiper belt also solves another mystery. Stern (1995b) suggests that it is not possible for objects with radii of -30 km to form in the current Kuiper belt, at least by two-body accretion. The curi ent surface density is too small for that much mass to have accreted into a single body. However, such objects could indeed form in a Kuiper belt with several Earth masses of material.

Finally, the idea of a historically massive, Kuiper belt has important consequences for the early evolution of the Pluto-Charon system (cf. Levison and Stern 1995). A massive Kuiper belt could be responsible for trapping Pluto into the 2:3 mean motion and Kosai resonances, In addition, it could help explain how the Pluto-Charon binary fortned by increasing the likelihood of a massive impact.

At heliocentric distances >50 AU, the Kuiper belt like] y consists of a population of icy planetesimals that may have orbited essentially undisturbed since the origin of the planetary system, though likely also modified by co] I i sional processes. If the r^2 surface density dependence holds to larger distances, then there are -2 x 10^9 comets between 50 and 100 AU, -4 x 10^{10} cornets between 100 and 500 AU, and 2 x 1010 comets between 500 and 1000 AU (if the disk extends that far), The total mass between 50 and 1,000 AU would be -0.4 $M_\oplus$. Somewhat more mass may exist in the Kuiper belt if the surface density distribution in the solar nebula was shallower than $1/r^2$.

The fact that the orbital element distribution of known Kuiper belt objects is different that what is expected from numerical integrations is another mystery, In particular, there is a problem with the region: $36 \leq a \leq 39$ AU, with $i \leq 15°$ and $e \leq 0.05$, which is dynamically stable for the age of the solar system. Discoveries to date suggest that this region is either partially or total] y unpopulated. If this result is confirmed by further observations, then some mechanism other than the long-term gravitational effects of the planets in their current configuration must have cleared it. This result may provide important and exciting clues to the formation and early evolution of the outer solar system.

The Oort cloud plays a less important role in the trans-Neptunian region than the Kuiper belt, though not a negligible one. Progress in understanding the dynamics of the Oort cloud, and in particular the inner Oort cloud, has been relatively poor in recent years. The Kuiper belt has been a more attractive target for researchers because the dynamical problem is a bit more tractable, the objects in question are observationally accessible, and the perturbers of the Kuiper belt, the giant planets, are known and well parameterized. In contrast, the Oort cloud perturbers include the galactic tide and random passing stars (in addition to the giant planets); the galactic tide is not well quantified (to within a factor of - 2), while stellar perturbations can only be treated in a statistical manner. Nevertheless, improvements in modeling codes and CPU speeds should make significant progress possible on the Oort cloud problem in the coming years.

The question of the existence of the Neptune Trojans is another relevant one for this region of space. The Trojan problem is no more difficult than the Kuiper belt studies to date, and thus could be attacked with the same computational tools, as we have begun to do in this chapter. Observational searches will continue to set upper limits on the population of the Neptune Trojan regions, as well as those for Saturn and Uranus. Obviously, the discovery of Trojan-type librators in the outer planets region would c1o much to motivate new research in this area.

It should be noted that we have not discussed in detail two classes of objects which pass through the trans-Neptunian region. These. arc the shor t-period comets with aphelia beyond 30 AU (e.g., Halley, Swift-Tuttle), and the Centaurs; the latter include the outer solar system objects listed in Table 1. Levison and Duncan (personal communication) have estimated that the steady-state population of Centaur-like objects in the trans-Neptunian region is on the order of 10^7 objects. This is more than two orders of magnitude less than the number of Kuiper belt

comets in the same region (note that we define Centaurs as objects that are no longer in long-lived, stable orbits, and that are now being chaotically scattered by close planetary encounters). Thus, while their rate of impact in the Pluto-Charon system is likely non-negligible, it is certainly far below that expected for Kuiper belt comets. The same is like] y even more true for the short-period comets traversing this region, since the Oort cloud population from which they are likely derived is also on] y a modest i mpactor source on Pluto and Charon.

We have also omitted discussion of the solar system dust environment in the trans-Neptunian region. Collisions within the Kuiper belt (Stern 1995c), and sputtering by solar wind particles and galactic cosmic rays on the surfaces of the Kuiper belt objects, will provide an in *situ* dust source. In addition, micron-sized particles in the zodiacal cloud from comets and asteroids will be blown outward through the region, while larger, centi meter-sized particles from collisions in the Oort cloud and the more distant regions of the Kuiper belt will spiral inward due to the Poynting-Robertson effect. Presumabl y, Pluto and Charon will sweep up some of this material at a predictable rate. Cometary meteoroids from Halley-type short-period comets will also contribute to the flux at 100 μm to centimeter sizes.

The discovery of objects at trans-Neptunian distances appears to be accelerating, with 1 found in 1992, 5 in 1993, 12 in 1994, and $\sim$40 in the first half of 1995 (including the HST discoveries), When the first asteroid, Ceres, was discovered in 1801, it was followed by three discoveries in the next six years, but then none for 38 years until the introduction of improved star charts and improved micrometers, and later, astronomical photography. As with the asteroids, the discovery of Kuiper belt objects appears to be closely associated with an enabling technology, the application of large area, low noise CCD's to astronomical searches. Further developments such as arrayed CCD focal planes, the new generation of very large telescopes, the next generation of HST instruments, and automated search programs should further accelerate the discovery rate in the near future. As the limiting magnitude of these searches improves, it will be interesting to see if they are also able to detect Oort cloud comets transiting this region, and inner Oort cloud comets passing through perihelion.

As a final note, we point out that the very slow heliocentric motion of comets in the Kuiper belt requires repeated astrometric observations over a period of many years to establish good orbital solutions for each object. observers are encouraged to support such programs so that the radial distribution and orbital statistics of the Kuiper belt can be established, and in

order to discriminate between different possible. dynamical resonances with Neptune, Physical observations of these objects are also of the highest priority, so that we may begin to understand the nature of this unique population.

Acknowledgment: We thank Brian Marsden for extensive discussions on the discovered Kuiper belt objects and their possible orbits, and George Wetherill for valuable discussions on size distributions. In addition, we are grateful to Martin Duncan for extensive discussions on Kuiper belt dynamics, and Alan Stern for discussions cm collisions. We also thank David Jewitt for the usc of his image of 1993 FW. This work was supported by the NASA Planetary Geology and Geophysics Program and the Origins of Solar Systems Program. It was performed, in part, at the Jet Propulsion Laboratory under contract with the National Aeronautics and Space Administration.

References

Anderson, J. D., and Standish, E. M., Jr. 1986. Dynamical evidence for Planet X. In *The* Galaxy *and the Solar System*, eds. R. Smoluchowski, J. N. Bahcall, and M. S. Matthews (Tucson:Univ. Arizona Press), pp. 286-296.

Anderson, J. D., Lau, E. 1.., Krisher, T. P., Dicus, D. A., Rosenbaum, D. C., and Teplitz, V. L. 1995. Improved bounds on non-luminous matter in solar orbit. *Ap. J.* in press.

Bailey, M. A., and C. R. Stagg 1988. Cratering constraints on the inner Oort cloud and implications for cometary origins. *Mon. Not. Roy. Astron. Sot. 235:1-32.*

Bowell, E. 1991. 1990 MB: The first Mars Trojan, In *Reports of Planetary Astronomy* (NASA: Washington), p. 147.

Byl, J. 1983. Galactic perturbations on nearly parabolic cometary orbits. *Moon & Planets 29:121-137.*

Campins, H., Telesco, C. M., Osip, D. J., Rieke, G. H., Rieke, M. J., and Schulz, B. 1994. The color temperature of 2060 Chiron: A warm and small nucleus, *Astron. J. 108:2318-2322.*

Cochran, A. L., Cochran, W. B., and Torbett, M. V. 1991. A deep imaging search for the Kuiper disk of comets. *Bull. Amer. Astron. Sot. 23:1314* (abstract).

Cochran, A., Levison, H., Stern, S. A., and Duncan, M. J. 1995. The discovery of Halley-sized Kuiper bch objects using HST. *Ap. J. Lett.*, in press.

Delsemme, A. H., and Patmiou, M. 1986. Galactic tides affect the Oort cloud: An observational confirmation. In *20th ESLAB Symposium on the Exploration of Halley's Comet, eds.* B. Battrick, E. J. Rolfe, and R. Reinhard, ESA SP-250, 2:409-412.

Dories, 1.., Levison, H., Duncan, M. 1995. On the dynamical lifetimes of planet-crossing objects. In *Completing the Inventory of the Solar System, d. E.* Bowel 1, in press.

Duncan, M., Quinn, T., and Tremaine, S. 1987. The formation and extent of the solar system comet cloud. *Astron. J. 94:1330-1338.*

Duncan, M., Quinn, T., and Tremaine, S. 1988. The oi igin of short-period comets. *Astrophys. J. 328:* L69-L73.

Duncan, M. J., Levison, H. F,, and Budd, S. M. 1995. The dynamical structure of the Kuiper belt. *Astron. J,,* submitted.

Edgeworth, K. E. 1949, The origin and evolution of the solar system. *Mon. Not. Roy. Astron. Sot. 109:600-609*

Everhart, E. 1967. Intrinsic distributions of cometary perihelia and magnitudes. *Astron. J. 72:1002-*1011,

Everhart, E. 1968. Change in total energy of comets passing through the solar system. *Astron. J.* **73**:1039-1052.

Everhart, E. 1973. Horseshoe and Trojan-type orbits associated with Jupiter and Saturn. *Astron. J.* **78**:316-328.

Fernández, J. A. 1980. On the existence of a comet belt beyond Neptune. *Mon. Not. Roy. Astron. Sot.* **192**:481-491.

Fernández, J. A. 1982. Dynamical aspects of the origin of comets. *A.wren. J.* 87:1318-1332.

Fernández, J. A. 1994. Dynamics of comets: Recent developments and new challenges. In *Asteroids, Comets, Meteors 1993, eds* A. Milani, M. Di Martino, and A. Cellino, (Dordrecht: Kluwer), pp. 223-240.

Fernández, J. A., and Ip, W.-H. 1987. lime dependent injection of Oort cloud comets into Earth-crossing orbits. *Icarus* 71:46-56.

Gladman, B., and Duncan, M. J. 1990. On the fates of minor bodies in the outer solar system. *Astron. J.* **100**:1680-1693.

Greenberg, R., Weidenschilling, S. J., Chapman, C. R., and Davis, D. R. 1984. From icy planetesimals to planets: Numerical simulations of collisional evolution. *Icarus* 59:87-113.

Hamid, S. E., Marsden, B. G., and Whipple, F. 1.. 1968. Influence of a comet belt beyond Neptune on the motions of periodic comets. *Astron. J.* 73:727-729.

Hartmarrn, W. 1969. Terrestrial, lunar, and interplanetary rock fragmentation. *Icarus* 10:201-213.

Heisler, J., and Tremaine, S. 1986. The influence of the galactic tidal field on the Oort comet cloud. *Icarus* 65, 13-26.

Hills, J. G. 1981. Comet showers and the steady-state infall of comets from the Oort cloud. *Astron. J.* **86**:1730-1740.

Hogg, D. W., Quinlan, G, D., and Tremaine, S. 1991. Dynamical limits on dark mass in the outer solar system. *Astron. J.* **101:2274-86.**

Holman, M. J., and Wisdom, J. 1993. Dynamical stability of the outer solar system and the delivery of short-period comets, *Astron. J. 105:1987-1999.*

Hut, P., Alvarez, W., Elder, W. P., Hansen, T., Kauffman, E. G., Keller, G., Shoemaker, E. M., and Weissman, P. R. 1987. Comet showers as possible causes of stepwise mass extinctions. *Nature* **329**:118-126.

Kuiper, G. P. 1951. On the origin of the solar system. In *Astrophysics, ed.* J. A. Hynek (New York: McGraw Hill), pp. 357-424.

Jewitt, D. 1991. Cometary photometry. in *Comets in the Post-Halley Era, eds,* R, L. Newburn, M. Neugebauer, and J. Rahe (Dordrecht:Kluwer), pp. 19-65.

Jewitt, D., and Luu, J. 1992. 1992 QB_1. *IAU Circular 5611.*

Jewitt, D., and Luu, J. 1993a. Discovery of the candidate Kuiper belt object 1992 QB_1. *Nature* **362**:730-732.

Jewitt, D., and Luu, J. 1993b. 1993 RO. *IAU Circular 5865*

Jewitt, D., and Luu, J. **1995.** The solar system beyond Neptune, *Astron. J.* **109:1867-1876.**

Knežević, Z., Milani, A., Farinella, P., Froeschle, Ch., and Froeschle, Cl. 1991. Secular resonances from 2 to 50 AU. *Icarus* 93:316-330.

Kowal, C. 1989. A solar system survey. *Icarus 77:118-123.*

Levison, H, F., and Duncan, M. J. 1990. A search for proto-comets in the outer regions of the solar system. *Astron. J.* **100:1669-1675,**

Levison, H. F., and Duncan, M, J. 1993. The gravitational sculpting of the Kuiper belt. *Astron. J.* **404**:L35-L38.

Levison, H. F., and Duncan, M. J. *1994.* The long-term dynamical behavior of short-period comets. *Icarus* 108:18-36.

Levison, H. 1995. Comet families. In *Completing the Inventory of the Solar System, ed.* E. Bowell, in press.

Levison, H., and Stern, S. A. 1995. Possible. origin and early dynamical evolution of the Pluto-Charon binary. *Icarus,* submitted.

Levison, H., Shoemaker, E. M., and Shoemaker, C. 1995. The dispersal of the Trojan swarm. In Hal's imagination.

LUU, J. X., and Jewitt, D. 1988. A two-part search for slow-moving objects. *Astron. J. 95:1256-1262.*

Luu, J., and Jewitt, D. 1993a. 1993 FW. *IAU Circular 5730.*

Luu, J., and Jewitt, D. 1993b. 1993 RP. *IAU Circular 5867*

Malhotra, R. 1993. The origin of Pluto's peculiar orbit, *Nature* 365:819-821.

Malhotra, R. 1995. The origin of Pluto's orbit: Implications for the solar system beyond Neptune. *Astron. J. 110:420-429.*

Marsden, B. G. 1992. 1992 QB_1, *IA U Circular 5684.*

Marsden, B. G. 1993a, 1992 QB_1. *1A U Circular 5855.*

Marsden, B. G. 1993b. 1993 FW. *IAU Circular 5856.*

Marsden, B. G, 1994. 1993 RO, 1993 RP, 1993 SB, 1993 SC. *IAU Circular 5983.*

Marsden, B. G. 1995. 1993 SC. *Min. Planet Elect. Circular* 1995-C17.

Marsden, B. G., Sekanina, Z., and Yeomans, D. K. 1973. Comets and nongravitational forces. V. *Astron. J. 78:211-225.*

Marsden, B. G., and William, G. V. 1995. *Catalogue of Cometary Orbits.* (Cambridge: Smithsonian Astrophysical Observatory), 108 pp.

Matese, J. J., Whitman, P. G., Innanen, K. A,, and Valtonen, M, J, 1995. Periodic modulation of the Oort cloud comet flux by the adiabatically changing galactic tide. *Icarus*, in press.

Mikkola, S., and Innanen, K. 1992. A numerical exploration of the. evolution of Trojan type asteroidal orbits. *Astron. J.* 104:1641-1649.

Mikkola, S., Innanen, K., Muinoen, K., and Bowell, E. 1994. A preliminary analysis of the orbit of the Mars Trojan asteroid (S261) Eureka. *Celest. Mech. & Dynam. Astron.* 58:53-64.

Moons, M., and Morbidelli, A. 1995. Secular resonances in mean motion commensurabilities: The 4/1, 3/1, 5/2, and 7/3 cases. *Icarus* 114:33-50.

Morbidelli, A,, Thomas, F'., and Moons, M. 1995. The resonant structure of the Kuiper belt and the dynamics of the first five trans-Neptunian objects. *Icarus,* submitted.

Morbidelli, A., Moons, M. 1993. Secular resonances in mean motion commensurabilities - The 2/1 and 312 cases, *Icarus* **102:316-332.**

Oort, J. H, 1950. The structure of the cloud of comets sun ounding the solar system and a hypothesis concerning its origin. *Bull. Astron. Inst. Neth. 11:91-110.*

Quinn, T., Tremaine, S., and Duncan, M. 1990. Planetary perturbations and the origin of short-period comets. *Astrophys. J.* 355:667-679.

Rahe, J., Vanysek, V., and Weissman, P. 1995. Properties of cometary nuclei. In *Hazards Due to Comets and Asteroids*, ed. T. Gehrels (Tucson: Univ. Arizona Press), pp. 597-634.

Roemer, E. 1965. Observations of comets and minor planets. *Astron. J.* 70:397-402.

Roemer, H., and Lloyd, R. E. 1966. Observations of comets, minor planets, and satellites, *Astron. J.* 71:443-457.

Roemer, E., Thomas, M., and Lloyd, R. E.1966. Observations of comets, minor planets, and Jupiter VIII. *Astron. J,* 71:591-601.

Shoemaker, E. M., and Wolfe, R. F. 1982. Cratering timescales for the Galilean satellites. In *Satellites of Jupiter, ed. D.* Morrison (Tucson: Univ. Arizona Press), pp. 277-339.

Standish, E. M. Jr, 1993. Planet X: No dynamical evidence in the optical observations. *Astron. J. 105:2000-2005.*

Stern, S. A. 1991. On the number of planets in the outer solar system: Evidence of a substantial number of 1000-km bodies. *Icarus* 90:271-281.

Stern, S. A. 1995a. The Kuiper disk. In *Completing the Inventory of the Solar System,* ed. E. Bowell, in press.

Stern, S. A, 1995b. Collisions in the Kuiper disk. I: Collision rates and their implications. *Astron. J.*, in press.

Stern, S. A. 1995c. Signatures of collisions in the Kuiper disk. *Astron. & Astrophys.,* submitted,

Tholen, D. J., Buie. M. W. 1995. The orbit of Charon. I. New Hubble Space Telescope observations. *Icarus,* submitted.

Tombaugh, C. 1961, In *Planets and Satellites, eds.* G Kuiper and B Middlehurst, (Chicago: Univ. Chicago Press), pp. 12-30.

Torbett, M. V. 1989. Chaotic motion in a comet disk beyond Neptune: The delivery of short-period comets. *AsIron. J. 98:1477-1481.*

Torbett, M. V., and Smoluchowski, R. 1990. Chaotic motion in a primordial comet disk beyond Neptune and comet influx. *Nature* 345:49-51.

Tremaine, S. 1990. Dark matter in the solar system. In *Baryonic Dark Mutter, eds.* D. Lynden-Bell and G. Gilmore (Dordrecht: Kluwer), pp. 37-65.

Tyson, J. A., Guhathakurta, P., Bernstein, G. M,, and Hut, P. 1992. limits on the surface density of faint Kuiper belt objects. *Bull. Amer. Astron. Sot. 24:1127* (abstract).

Weissman, P. R. 1977. Initial energy and perihelion distributions of Oort cloud comets. In *Comets, Asteroids, Meteorites: Interrelations, Evolution, and Origins,* ed. A. H. Delsemme, (Toledo: Univ. Toledo Press), pp. 87-91.

Weissman, P. R. 1979. Physical and dynamical evolution of long-period comets. In *Dynamics of the Solar System, ed.* R. L. Duncombe (Dordrecht: D. Reidel), pp. 277-282.

Weissman, P. R, 1985. Dynamical evolution of the Oort cloud. In *Dynamics of Comets: Their Origin and Evolution,* eds. A. Carusi and G. D. Valsecchi (Dordrecht: D. Reidel), pp. 87-96.

Weissman, P. R. 1990. The cometary impactor flux at the Earth. in *Global Catastrophes in Earth History, eds.* V. L. Sharpton and P. D. Ward, Geological Society of America Special Paper 247, pp. 171-180.

Weissman, P. R, 1991. Dynamical history of the Oort cloud, In *Comets in the Post-Halley Era,* eds. R. L. Newburn Jr., M. Neugebauer, and J. Rahe (Dordrecht: Kluwer), 1:463-486.

Weissman, P. R. 1993. No, we are not in a cometary shower. *Bull. Amer. Astron Sot. 25:1063* (abstract).

Weissman, P. R. 1995a. The Kuiper belt. in *Annual Reviews of Astronomy and Astrophysics,* (Palo Alto: Annual Reviews), in press,

Weissman, P. R. 1995b. Star passages through the Oort cloud. In *Small Bodies in the Solar System and their Interactions with the Planets, ed.* H. Rick man (Dordrecht: Kluwer), in press.

Weissman, P. R., and Wetherill, G. W. 1974. Periodic Trojan-type orbits in the Earth-Sun system. *Astron. J.* 79:404-412.

Weissman, P. R., Dobrovolskis, A. R., and Stern, S. A. 1989. Constraints on impact rates in the Pluto-Charon system and the population of the Kuiper comet belt. *Geophys. Res. Lett. 16:1241-1244.*

Weissman, P. R,, and Stern, S. A. 1994. The impactor flux in the Pluto-Charon system, *Icarus* 111:378-386.

Wetherill, G. W, 1975. Late heavy bombardment of the moon and terrestrial planets. In *Proc. 6th Lunar Sci. Conf.*, pp. 1539-1561.

Wetherill, G. W. 1991. End products of cometary evolution: Cometary origin of Earth-crossing bodies of asteroidal appearance. In *Comets in the Post-Halley Era, eds.* R. L. Newburn, M. Neugebauer and J. Rahe (Dordrecht: Kluwer), 1:537-556.

Wetherill, G. W., and Stewart, G. R. 1993. Formation of planetary embryos: Effects of fragmentation, low relative velocity, and independent variation of eccentricity and inclination. *Icarus* 106:190-209.

Whipple, F. L. 1964. Evidence for a comet belt beyond Neptune. *Proc. Natl. A cad. Sci.* U.S. 51:711-718.

Williams, 1. P., Fitzsimmons, A., and O'Ceallaigh, D. 1993, 1993 SB and 1993 SC. *IAU Circular 5869.*

Wisdom, J,, and Holman, M, 1991. Symplectic maps for the N-body problem. *Astron. J.* 102:1528-1538.

Yeomans, D. K. 1986. Physical interpretations from the motions of comets Halley and Giacobini-Zinner. In *20th ESLAB Symposium on the Exploration of Halley's Comet*, eds. B. Battrick, E. J. Rolfe, and R. Reinhard, ESA SP-250, 2:419-425.

Table 1. Outer Solar System Planet-Crossing Objects"

Designation	a AU	e	q AU	Q AU	i deg	P yr	H mag	R+ km
2060 Chiron	13.73	0.384	8.46	19.00	6.93	50.85	6.0	95
5145 Pholus	2<0.36	0.573	8.69	32.03	24.70	91.85	7.3	60
1993 HA_2	24.78	0.523	11.8?	37.74	15,63	123,38	9.5	22
1994 TA	17.5	0.393	10.62	24.38	5.43	73.0	11.3	10
1995 DW_2	24.85	0.242	18.84	30.86	4.2	123.9	9.3	24
1995 GO	21.79	0.693	6.69	36.89	17.3	101,7	9,6	21

" Listed in order of discovery. Data from discovery 1 AU Circulars, Minor Planet Electronic Circulars.

+ Mean Chiron diameter measured by Campins et al. (1994). Other diameters are estimated based on an assumed albedo of 0.10.

Table 2. Kuiper Belt Objects"

Designation	r AU	a AU	e	i deg.	P yr	R mag.	R km
1992 QB_1	41.2	43.83	0.088	2.21	290.2	22.8	130
1993 FW	42.4	43,93	0.041	7.74	291.2	22.8	140
1993 RO	32.3	39.70'	0.205+	3.72	250.1	23	70
1993 RP	35.4			2.79		24.5	50
1993 SB	33,1	39.42'	0.321+	2.28	247.5	22.7	9 0
1993 SC	34.4	39.47	0.180	5.16	248.0	21,7	150
1994 ES_2	46.2	45.93	0.125	1.05	311.3	24.3	80
1994 EV_3	44.8	43.07	0.038	1.68	282.6	23.3	120
1994 GV_9	42.2	43,39	0.042	0.547	285.8	23.1	120
1994 JS	36.6	42.84#	0.234#	14.0	280.4	23.1	80
1994 JV	35.2			18.1		22.4	110
1994 JQ_1	43.4	44.31	0,027	3,73	295.0	22.9	140
1994 JR_1	35.2	39.76'	0.130+	3.80	250.7	22.5	110
1994 TB	31,7	36.56	0.157	12.1	221.1	21.5	140
1994 TG	42.2			6.76		23	120
1994 TH	40.9			16.1		23	120
1994 TG_2	42.4			2.25		24	80
1994 VK_8	43.4			1.43		22.3	180
1995 DA_2	34.0	36.34!	0.116'	6.59	219.1	23.0	70
1995 DB_2	40.6	43.49#	0.067#	4.27	286,8	22.5	140
1995 DC_2	45.2			2.14		22.5	180
1995 FB_{21}	42.4			0.67		23.1	110
1995 GJ	39.0	42.91#	0.091#	22.9	281.1	22.5	130
1995 GA_7	37.9	39.46'	0.119+	3.54	247.8	23	100
1995 GY_7	41.3			0.94		23,5	100
1995 HM_5	32.5	39.53'	0.178+	4.70	248.6	23.1	70
1995 KJ_1	43.2			3.80		22.5	160
1995 KK_1	32.8	39.47'	o. 190+	9.25	248.0	23.0	70

* Listed in order of discovery. Data from discovery IAU Circulars, Minor Planet Electronic Circulars, and B. Marsden (personal communication).

+ Tentative orbit. Forced 2:3 resonance solution.

' Tentative orbit. Forced 3:4 resonance solution,

Tentative orbit. Forced 3:5 resonance solution.

Table 3. Constraints on the Kuiper Belt Population

Source	Size Range km	Number $30 < r < 50$ AU	Reference
1, Short-period comet supply	$1 \leq R \leq 10$	$\sim 5 \times 10^9$	Duncan et al. (1995)
2. HST observations	$6 \leq R \leq 12$	$> 2 \times 10^8$	Cochran et al. (1995)
3. Pluto-Charon perturbers	$R \geq 20$	$< 3 \times 10^7$	Levison and Stern (1995)
4. Ground-based searches	$50 \leq R \leq 200$	$> 3.5 \times 10^4$	Jewitt and Luu (1995)
5. Pluto	$R \geq 1{,}000$	1	Tombaugh (1961), Kowal (1989)
6. Collisional theory	$R < 0.5$?	0	Stern (1995)

Figure captions

Figure 1. Discovery image of 1993 FW (inside the box) taken March 28, 1993 with the University of Hawaii 2.2 m telescope on Mauna Kea by Luu and Jewitt (1993a). The comet is about R magnitude 23.3; the bright star at lower right is about magnitude 16. The vertical streak at the left is an artifact from the Tektronix 2048 x 2048 CCD. South is at the top; west is at the left.

Figure 2, Cumulative absolute R magnitude distribution for the 28 discovered Kuiper belt comets (solid curve), and for just the 16 objects discovered at $r \geq 40$ AU (dashed curve). The diameter scale assumes a cometary albedo of 0.04. The flattening of the distribution at magnitudes > 7.0 is due to observational incompleteness,

Figure 3. Perihelion distribution of dynamically new, long-period comets from the Oort cloud, as found by Weissman (1985). Jupiter and Saturn serve as a dynamical barrier to the diffusion of cometary perihelia into the inner planets region.

Figure 4. The dynamical lifetime for test particles in the Kuiper belt derived from Duncan et al.'s (1995) 4 x 10^9 year integrations. Each particle is represented by a narrow vertical strip of color, the center of which is located at the particle's initial eccentricity and semimajor axis (initial inclination = 1°). The color of each strip represents the dynamical lifetime of the particle. Strips colored yellow represent objects that survive for the length of the integration, 4 x 10^9 years. Dark regions are particularly unstable on these timescales. The green dots represent the location of the orbits for the known Kuiper belt objects, as determined by Marsden. For reference, the locations of the important Neptune mean motion resonances are shown in blue and two curves of constant perihelion distance, q, are shown in red.

Figure 5. The dynamical lifetime for test particles with initial eccentricity = 0.01 derived from Duncan et al.'s (1995) 10^9 year integrations. This plot is similar to Figure 4 except that a different color table was used for the solid bars. In addition, the red and yellow curves show the locations of Neptune longitude of perihelion secular resonances (ν_8) and the Neptune longitude of the ascending node secular resonances (ν_{18}), respectively, as determined by Knežević et al. (1991). The green lines show the location of the. important Neptune mean motion resonances.

Figure 6. The location of the Kozai and ν_{18} secular resonances for objects currently trapped in the 2:3 mean motion resonance with Neptune, as determined by Morbidelli et al, (1995). This plot assumes that the 2:3 libration amplitude is small and thus that a $\simeq$ 39,4 AU. The circles represent the location of the known Kuiper belt objects that lie in the 2:3 resonance.

Figure 7. The current radial distribution of comets in the Kuiper belt as determined by Duncan et al. (1995). Their model assumes that the surface density distribution initially follows a power law versus heliocentric distance with an exponent of -2 (shown as a dotted curve), and that all comets had the same initial inclination, i == 10, and eccentricity, e = 0.05. The model does not take into account the effects of dissipation, collisions, or the possible early radial migration of the giant planets.

Figure 8. The cumulative number of objects in the Kuiper belt between 30 and 50 AU, larger than radius R as a function of R. The filled circles indicate the known constraints as listed in Table 3, and arrows indicate upper/lower limits. 'l'he dotted blue box represents the uncertainties in Duncan et al.'s (1995) estimate of the number of Kuiper belt objects required to provide the observed flux of short-period comets. Each labeled straight line indicates a power law size distribution that has been fit to a narrow range of radii (indicated by the bold line), but for purposes of comparison, we plot it for all sizes. The blue line labeled 'A' is a power law of slope q= 3 (consistent with Shoemaker' and Wolfe's 1982 estimate of q for comets) that has 5 x 109 objects with radii between 1 and 10 km (consistent with Duncan et al,'s 1995 estimate). The green lines labeled 'B' and 'C' are power laws derived from Cochran et al.'s (1995) estimate of >2 x 108 objects with radii between 6 and 12 km, and q =3 and q =5, respectively. The red lines labeled 'I)' and 'E' are derived from Jewitt and Luu's (1995) estimate of 3.5 x 10^4 objects with radii between 50 and 200 km, and q =2 and q='1, respectively. The black curve represents a broken power law as suggested for the cometary population by various researchers (see text).

Figure 9, Cumulative mass distributions for a runaway growth model for the inner solar system as calculated by Wetherill and Stewart (1993). This is a reproduction of their Figure 1.

Figure 10, The stable regions around the Neptune Trojan points as determined by Holman and Wisdom (1993). A point is plotted for each particle that survived the full 2 x 10^7 year integration. The axes are the particle's initial displacement in mean longitude from Neptune and the ratio of the particle's semimajor axis to Neptune's semimajor axis. A two-dimensional stable region exists near each of the triangular Lagrange points. Note., however, the asymmetry between the L_4 and L_5 regions.

Figure 11, Contour plot of the dynamical lifetimes of Neptune Trojans as a function of their initial proper eccentricity, e_p, and libration amplitude, D.

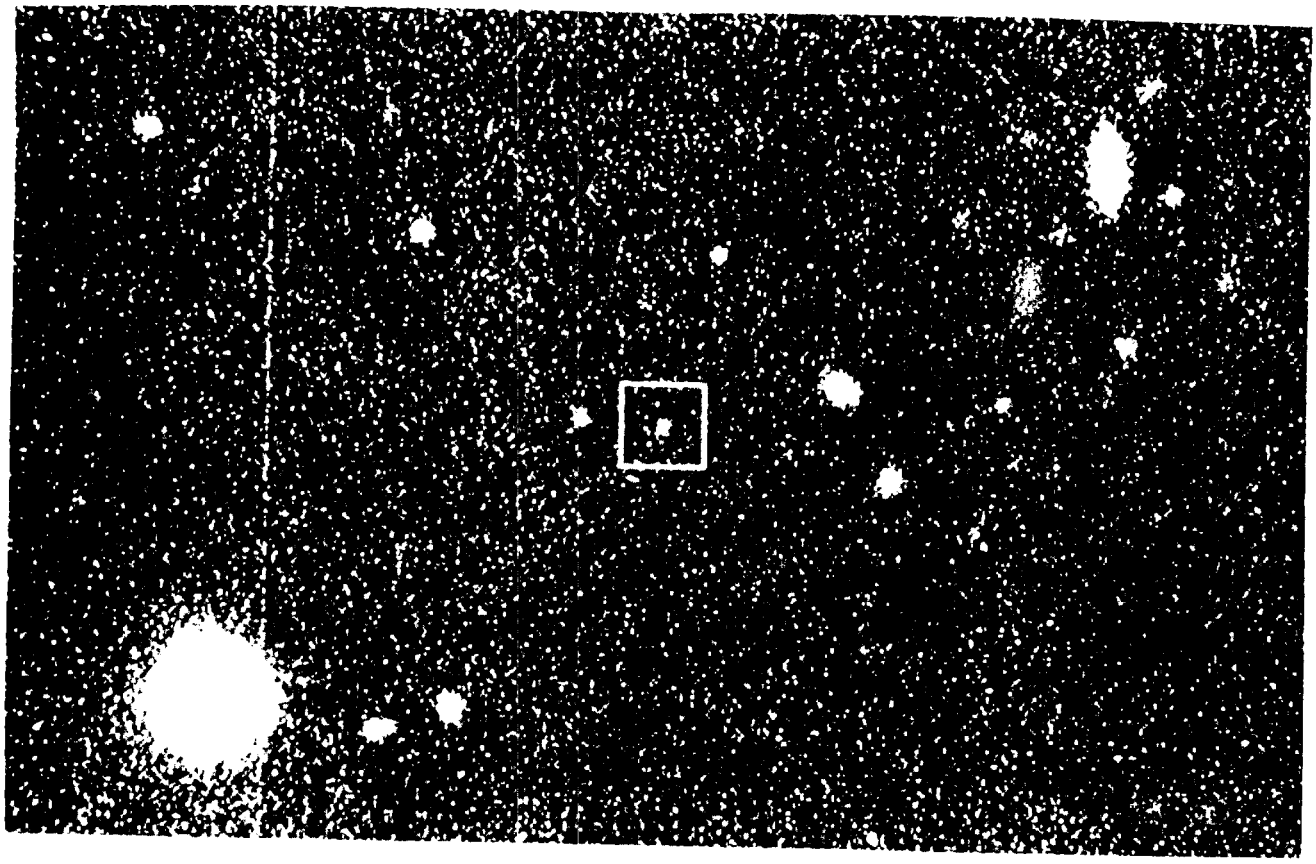

Figure 1

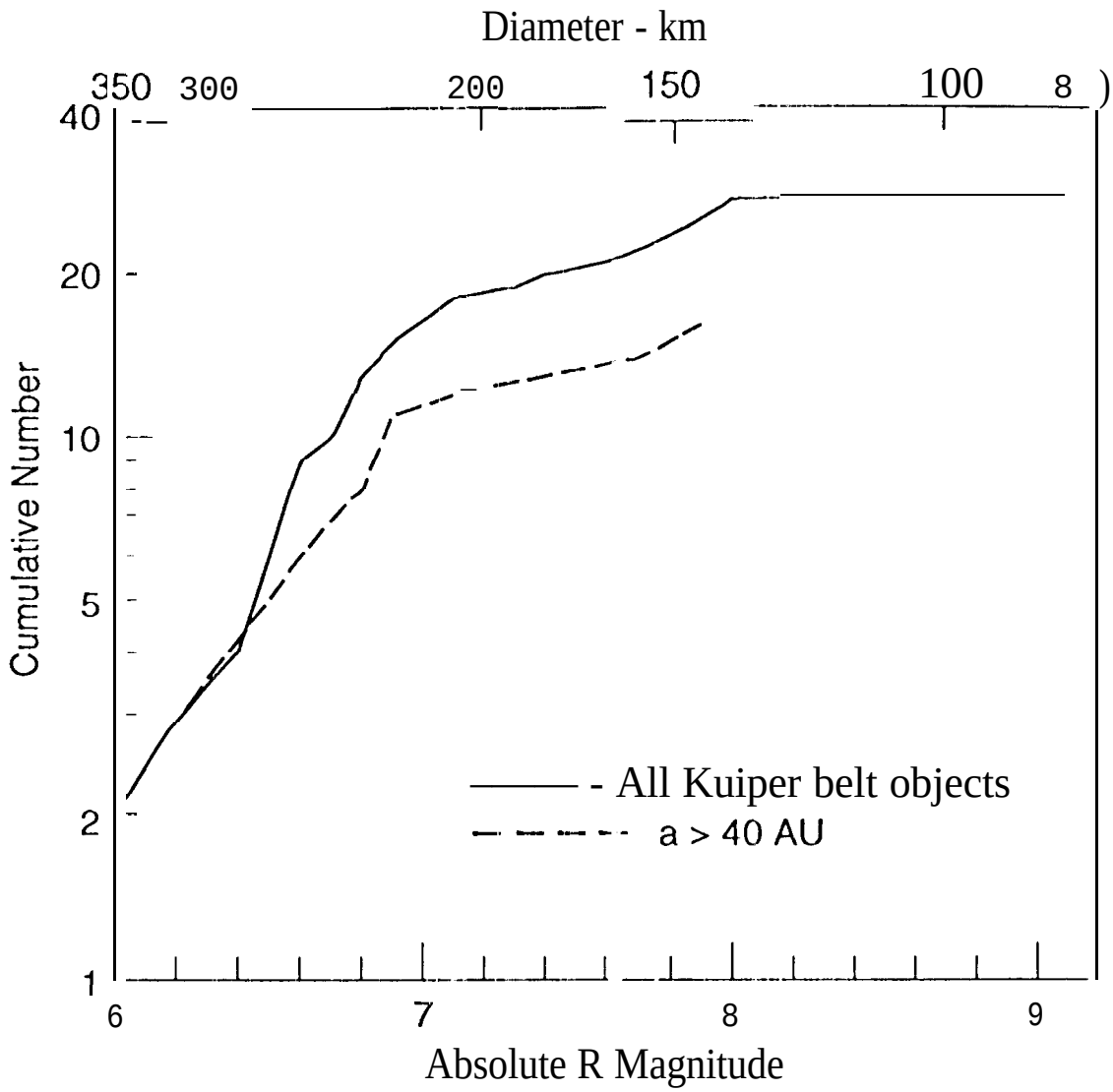
Diameter - km
350
300
200
150
100
8
40
20
10
5
2
1
Cumulative Number
- All Kuiper belt objects
a > 40 AU
6
7
8
9
Absolute R Magnitude

Figure 2

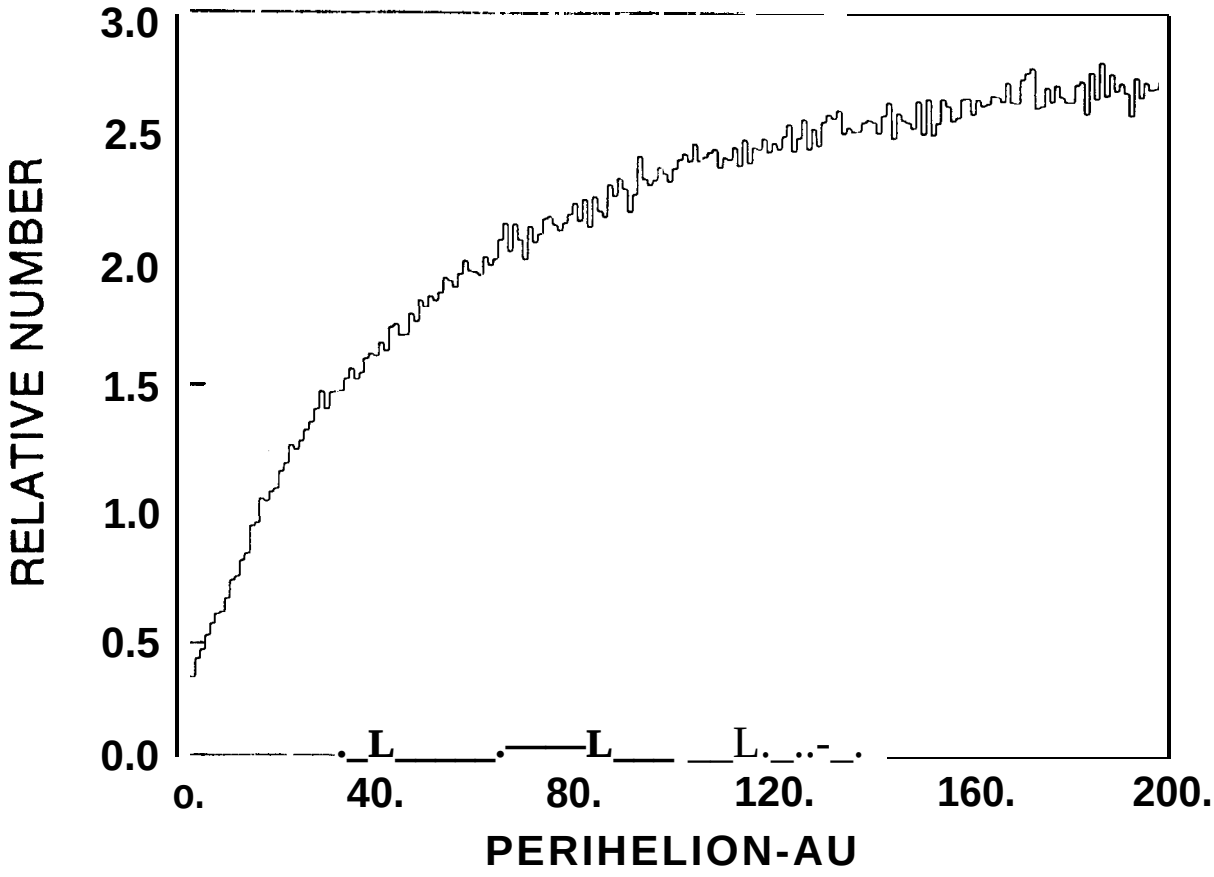
RELATIVE NUMBER
3.0
2.5
2.0
1.5
1.0
0.5
0.0
0.
40.
80.
120.
160.
200.
PERIHELION-AU

Figure 3

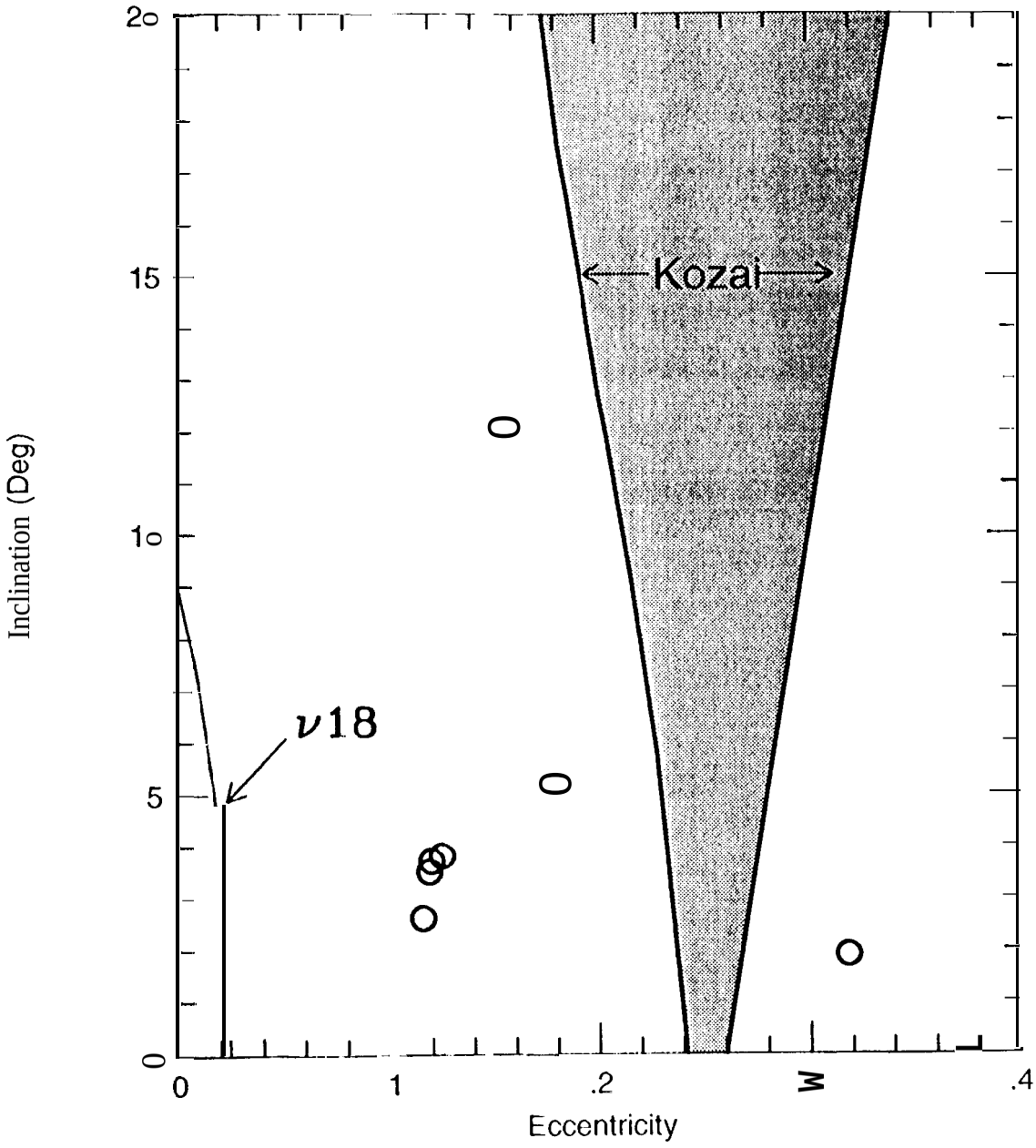

Figure 6

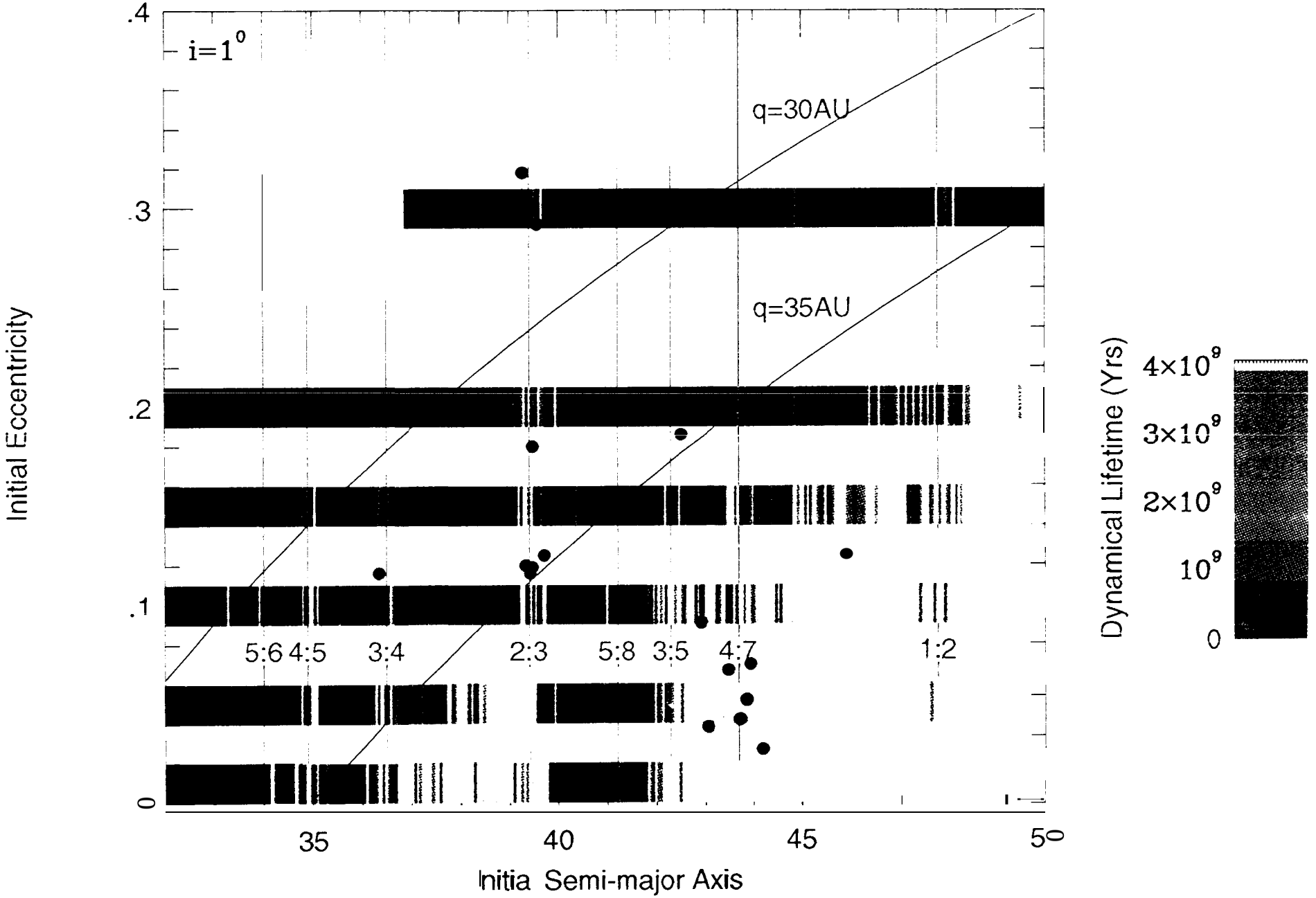
i=1°
q=30AU
q=35AU
5:6
4:5
3:4
2:3
5:8
3:5
4:7
1:2
.4
.3
.2
.1
0
35
40
45
50
Initia Semi-major Axis
Initial Eccentricity
Dynamical Lifetime (Yrs)
4×10^9
3×10^9
2×10^9
10^9
0

inc(deg.)
0
20
40
60
80
3:4
5:7
2:3
3:5
36
38
40
42
a(AU)
Dynamical Lifetime (Yrs)
0
2×10^8
4×10^8
6×10^8
8×10^8

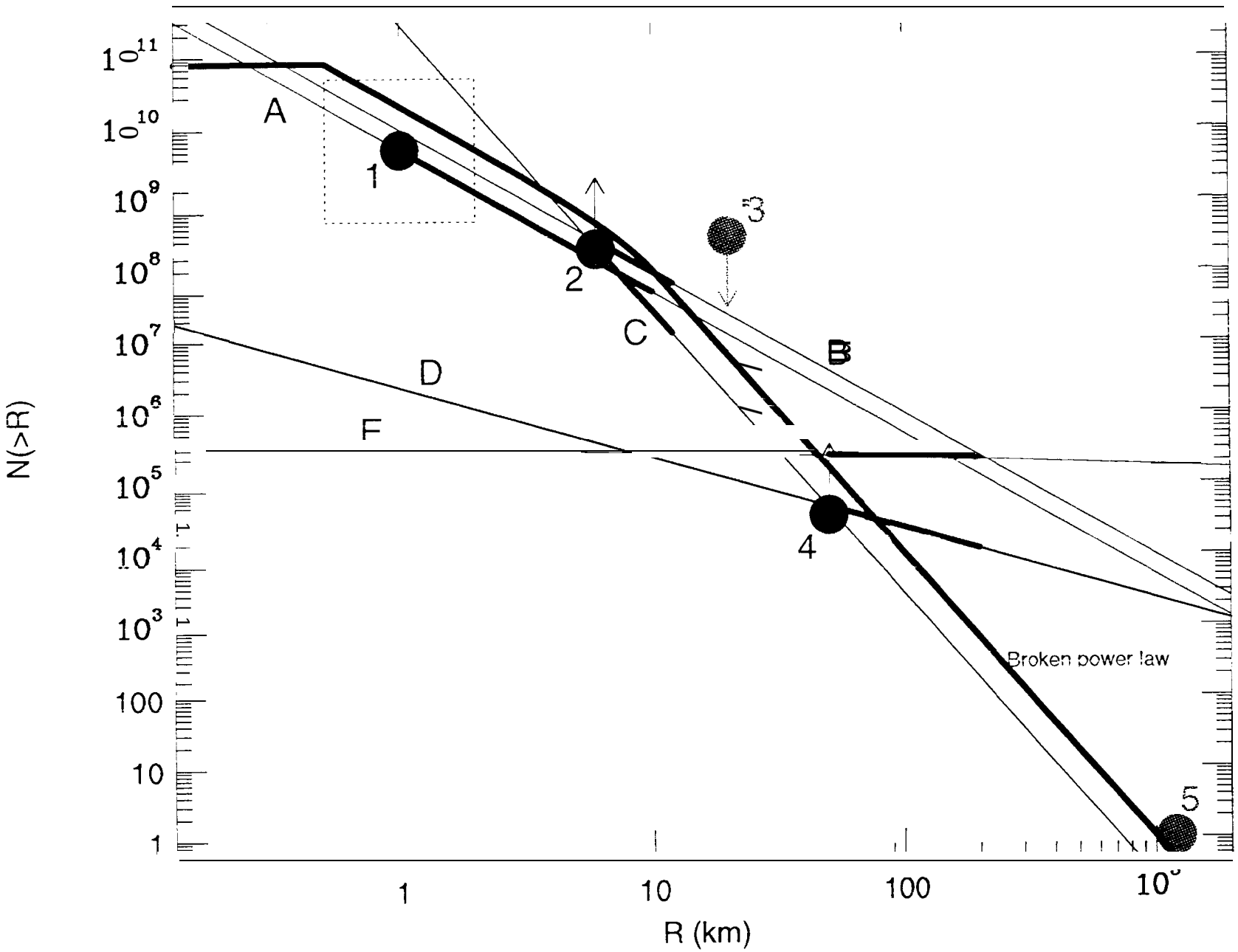
N(>R)
10^{11}
10^{10}
10^{9}
10^{8}
10^{7}
10^{6}
10^{5}
10^{4}
10^{3}
100
10
1
A
1
2
3
C
B
D
F
4
5
Broken power law
1
10
100
R (km)

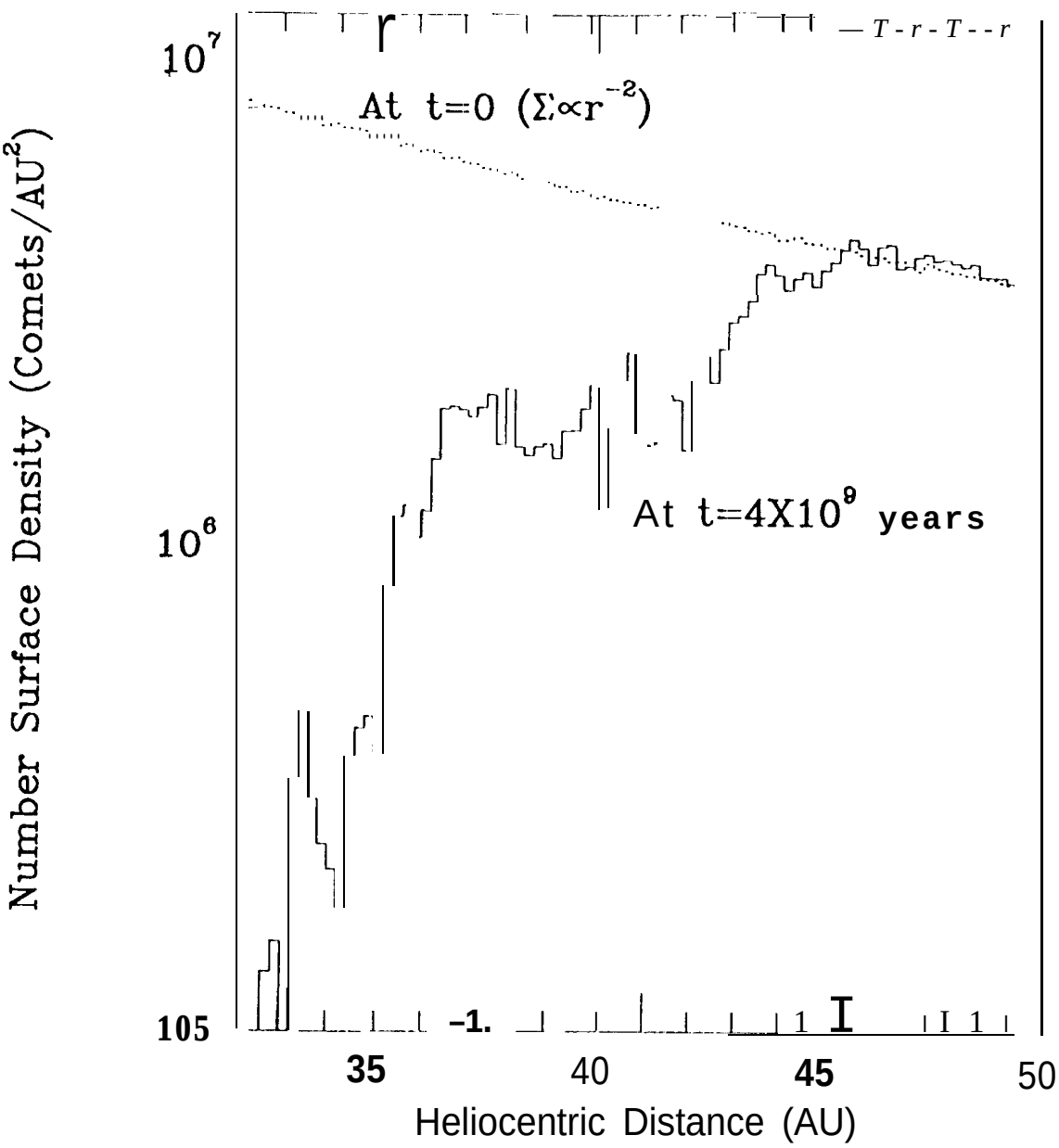
Number Surface Density (Comets/AU²)
10⁷
10⁶
105
At t=0 (Σ∝r⁻²)
At t=4X10⁹ years
-1.
35
40
45
50
Heliocentric Distance (AU)

Figure 7

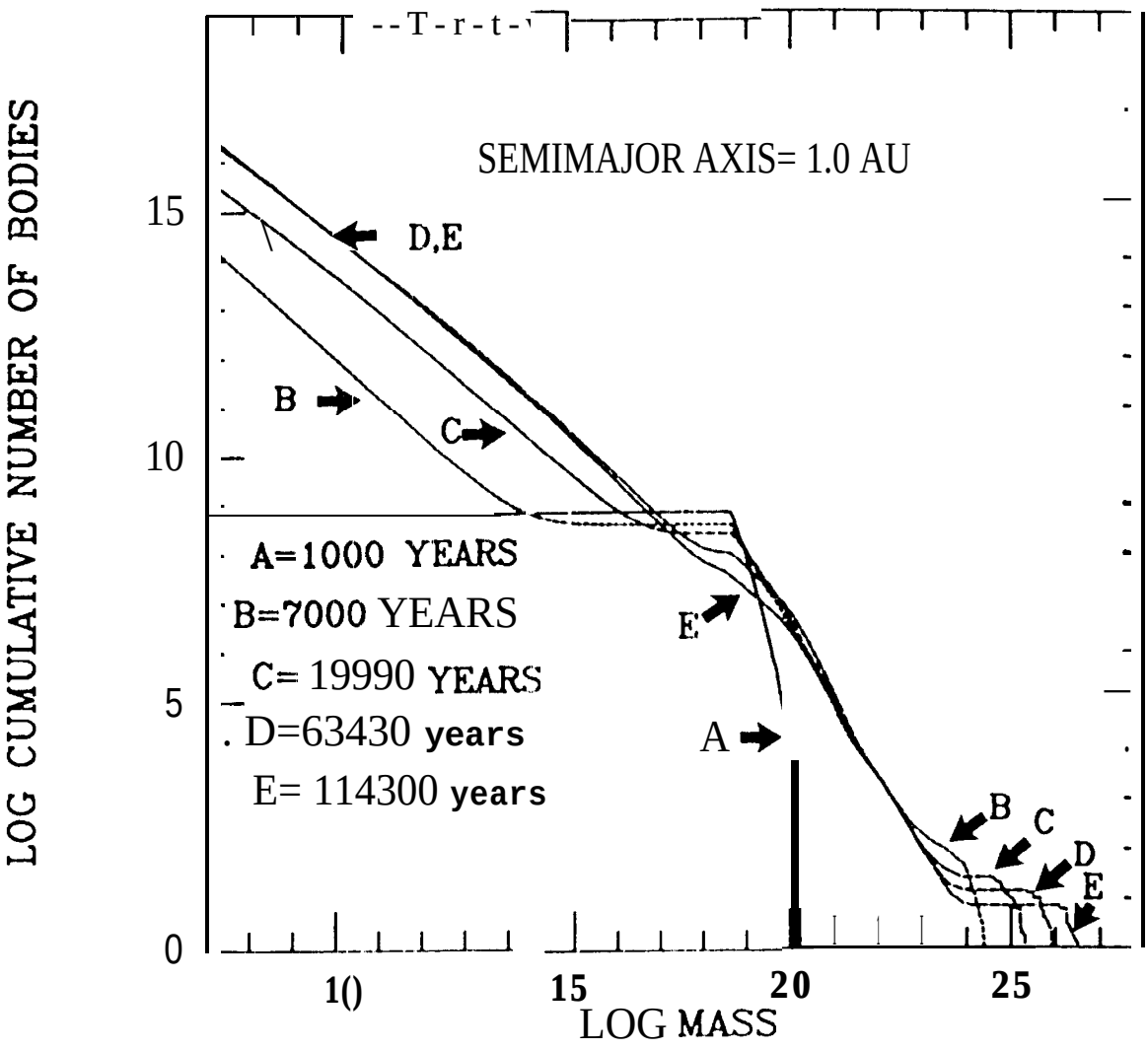
SEMIMAJOR AXIS= 1.0 AU
LOG CUMULATIVE NUMBER OF BODIES
LOG MASS
15
10
5
0
15
20
25
D,E
B
C
A=1000 YEARS
B=7000 YEARS
C= 19990 YEARS
D=63430 years
E= 114300 years
E
A
B
C
D
E

Figure 9

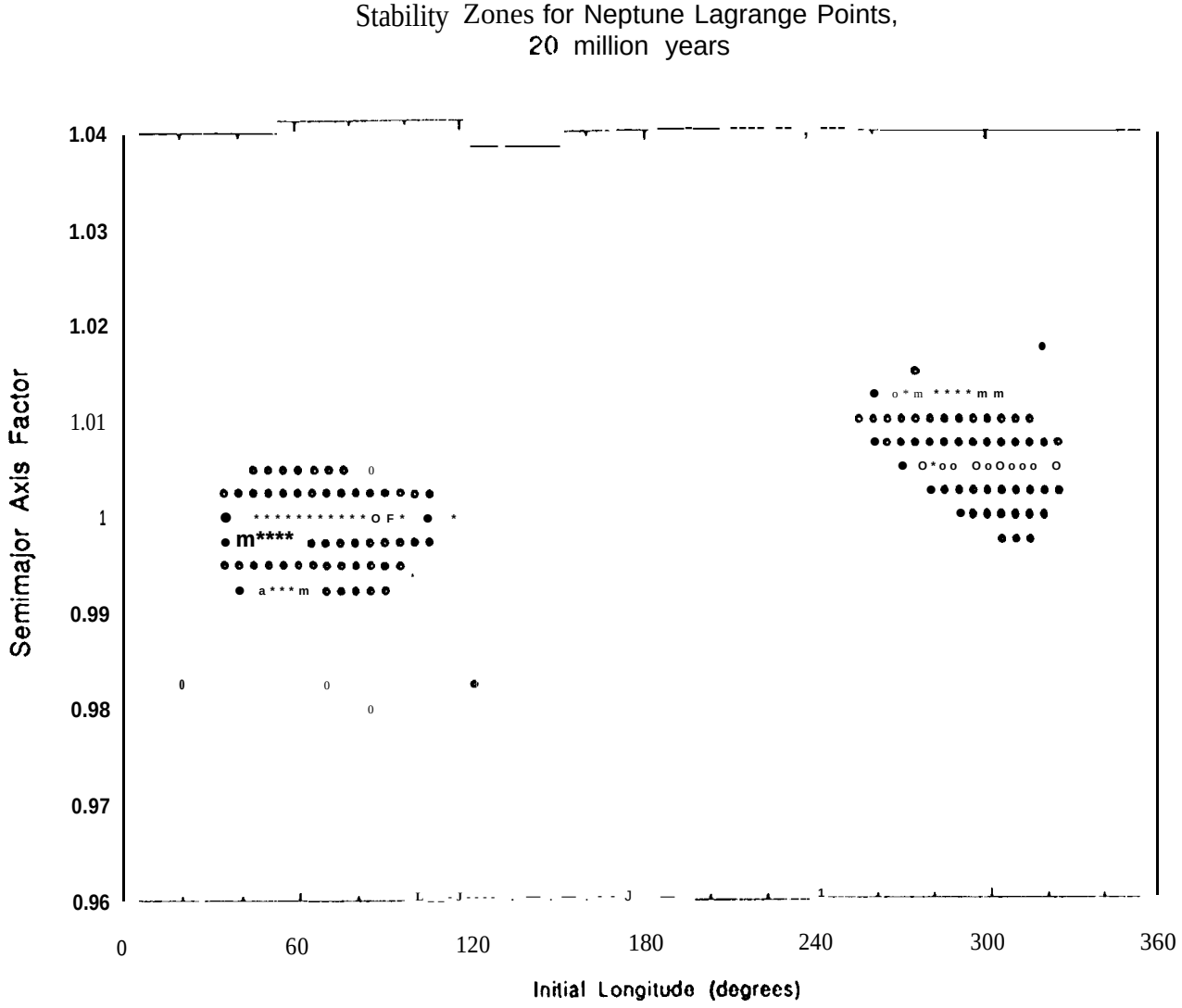
Stability Zones for Neptune Lagrange Points,
20 million years
Semimajor Axis Factor
1.04
1.03
1.02
1.01
1
0.99
0.98
0.97
0.96
0
60
120
180
240
300
360
Initial Longitude (degrees)

Figure 10

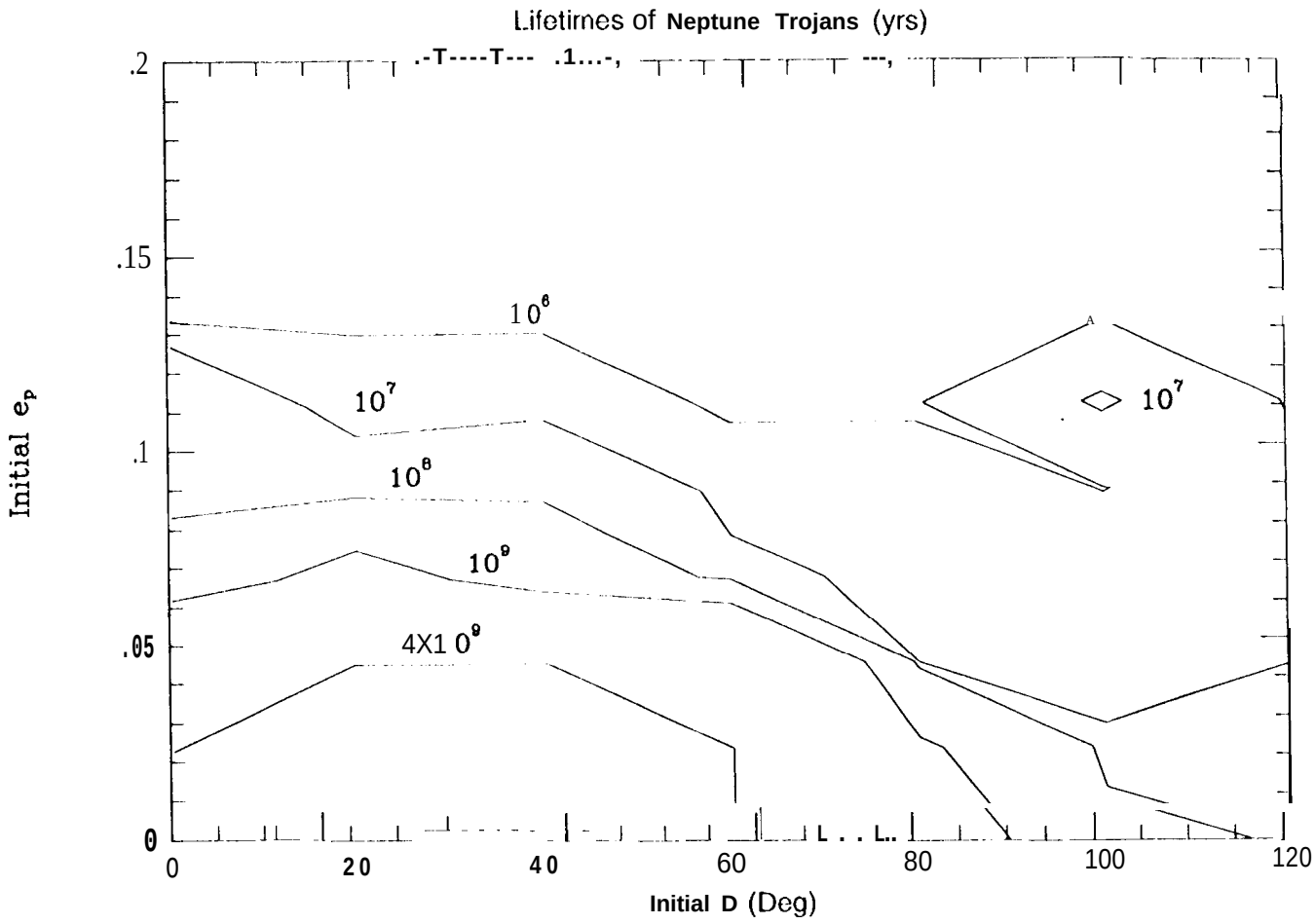
Lifetimes of Neptune Trojans (yrs)
.2
.15
.1
.05
0
Initial e_p
10^6
10^7
10^8
10^9
4X1 0^9
10^7
0
20
40
60
80
100
120
Initial D (Deg)

Figure 11